7 Resistivity Logs

The resistivity of a formation is a key parameter in determining hydrocarbon saturation. Electricity can pass through a formation only because of the conductive water it contains. With a few rare exceptions, such as metallic sulfide and graphite, dry rock is a good electrical insulator. Moreover, perfectly dry rocks are very seldom encountered. Therefore, subsurface formations have finite, measurable resistivities because of the water in their pores or absorbed in their interstitial clay.

The resistivity of a formation depends on:

- Resistivity of the formation water.
- Amount of water present.
- Pore structure geometry.

The resistivity (specific resistance) of a substance is the resistance measured between opposite faces of a unit cube of that substance at a specified temperature. The meter is the unit of length and the ohm is the unit of electrical resistance. In abbreviated form, resistivity is

$$R = r\,A/L\,, \qquad \text{(Eq. 7-1)}$$

where

R is resistivity in ohm-meters,

r is resistance in ohms,

A is area in square meters,

and

L is length in meters.

The units of resistivity are ohm-meters squared per meter, or simply ohm-meters (ohm-m).

Conductivity is the reciprocal of resistivity and is expressed in mhos per meter. To avoid decimal fractions, conductivity is usually expressed in millimhos per meter (mmho/m), where 1000 mmho/m = 1 mho/m:

$$C = \frac{1000}{R}\,. \qquad \text{(Eq. 7-2)}$$

Formation resistivities are usually from 0.2 to 1000 ohm-m. Resistivities higher than 1000 ohm-m are uncommon in permeable formations but are observed in impervious, very low porosity (e.g., evaporites) formations.

Formation resistivities are measured by either sending current into the formation and measuring the ease of the electrical flow through it or by inducing an electric current into the formation and measuring how large it is.

CONVENTIONAL ELECTRICAL LOGS

During the first quarter-century of well logging, the only resistivity logs available were the conventional electrical surveys. Thousands of them were run each year in holes drilled all over the world. Since then, more sophisticated resistivity logging methods have been developed to measure the resistivity of the flushed zone, R_{xo}, and the true resistivity of the uninvaded virgin zone, R_t.

The conventional electrical survey (ES) usually consisted of an SP, 16-in. normal, 64-in. normal, and 18-ft 8-in. lateral devices. Since the ES log is the only log available in many old wells, the measurement principles and responses are covered in this section. For more detailed information on old electric logs, refer to Ref. 22.

Principle

Currents were passed through the formation by means of current electrodes, and voltages were measured between measure electrodes. These measured voltages provided the resistivity determinations for each device.

In a homogeneous, isotropic formation of infinite extent, the equipotential surfaces surrounding a single current-emitting electrode (A) are spheres. The voltage between an electrode (M) situated on one of these spheres and one at infinity is proportional to the resistivity of the homogeneous formation, and the measured voltage can be scaled in resistivity units.

Resistivity Devices

In the normal device (Fig. 7-1), a current of constant intensity is passed between two electrodes, A and B. The resultant potential difference is measured between two other electrodes, M and N. Electrodes A and M are on the sonde. B and N are, theoretically, located an infinite distance away. In practice, B is the cable armor, and N is an electrode on the bridle (the insulation-covered lower end of the cable) far removed from A and M. The distance AM is called the spacing (16-in. spacing for the short normal, 64-in. spacing for the long normal), and the point of inscription for the measurement is at O, midway between A and M.

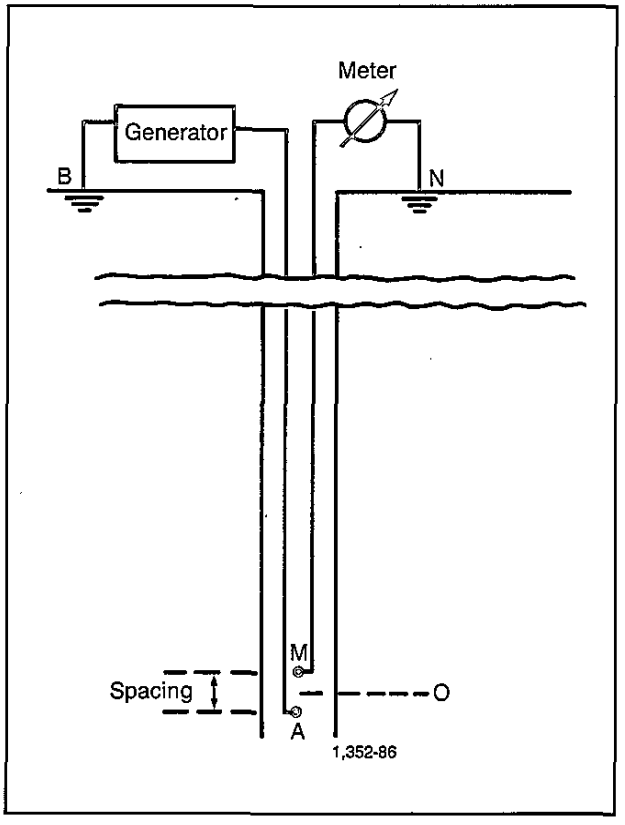

Fig. 7-1—Normal device—basic arrangement.

In the basic lateral device (Fig. 7-2), a constant current is passed between A and B, and the potential difference between M and N, located on two concentric spherical equipotential surfaces centered on A, is measured. Thus, the voltage measured is proportional to the potential gradient between M and N. The point of inscription is at O, midway between M and N. The spacing AO is 18 ft 8 in. The sonde used in practice differs from that shown in Fig. 7-2 in that the positions of the current and measuring electrodes are interchanged; this

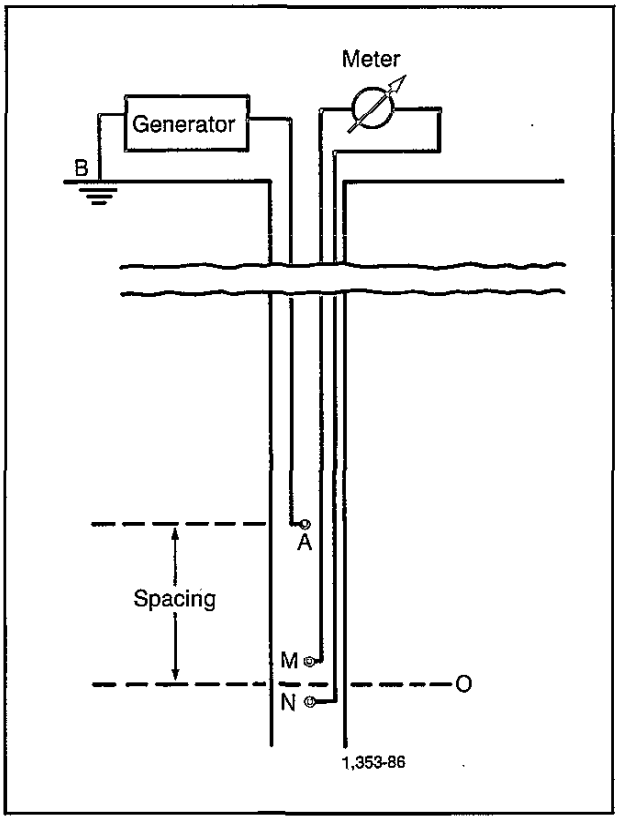

Fig. 7-2—Lateral device—basic arrangement.

reciprocal sonde records the same resistivity values as the basic sonde described above. Also, all electrodes are in the borehole, with N located 50 ft 10 in. above M.

Generally, the longer the spacing, the deeper the device investigates into the formation. Thus, of the ES resistivity logs, the 18-ft 8-in. lateral has the deepest investigation and the 16-in. normal the shallowest. In practice, however, the apparent resistivity, R_a, recorded by each device is affected by the resistivities and geometrical dimensions of all media around the device (borehole, invaded and uncontaminated zones, and adjacent beds).

Normal and Lateral Curves

In the following examples, the shapes of the normal and lateral curves are described for a few typical cases. All cases correspond to noninvaded formations. To read the conventional resistivity logs correctly, a knowledge of these typical curve shapes is required.

Fig. 7-3 illustrates the response of the normal device in beds more resistive than the surrounding formations. (The resistivities of the various media are indicated on the figure.)

The upper part shows the response in a thick bed (h = 10 AM). The curve is symmetrical and a maximum is observed at the center of the bed, where the reading is almost equal to R_t (no invasion). The apparent bed thickness on the normal curve is less than actual bed thickness by an amount equal to the spacing.

The lower part shows the response in a bed with a thickness less than the spacing. The curve is still symmetrical but is reversed. A minimum apparent resistivity, actually less than surrounding formation resistivity, is observed opposite the bed even though bed resistivity is greater than surrounding bed resistivity. Two spurious peaks appear, one above and one below the bed; the distance between the two peaks is equal to bed thickness plus the spacing of the normal.

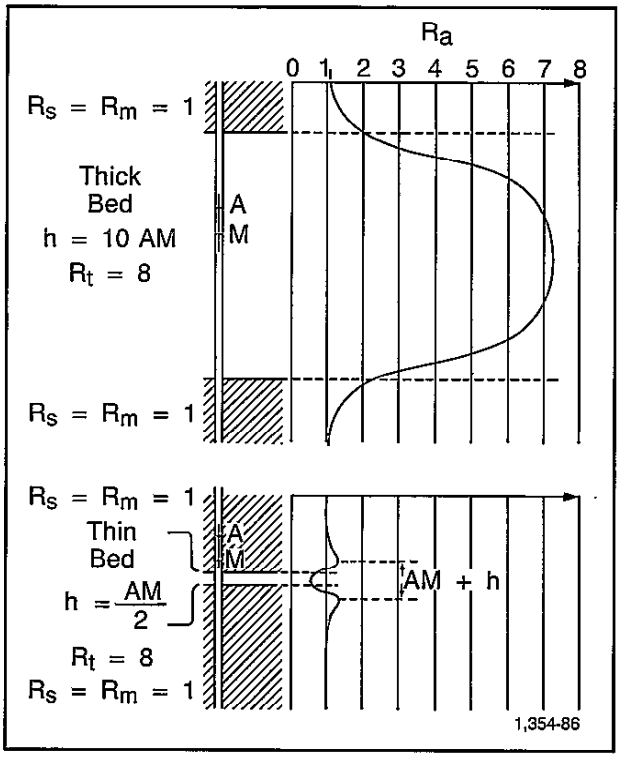

Fig. 7-3—Normal curves—bed more resistive than adjacent formations.

Fig. 7-4 illustrates the response of the normal device in thick and thin beds less resistive than the surrounding formations. The curves are symmetrical and the apparent bed thickness is greater than actual bed thickness by an amount equal to the AM spacing.

Fig. 7-5 illustrates the response of the lateral device in beds more resistive than the surrounding formations. Since the usual lateral spacing is 18 ft 8 in., the cases represented correspond to bed thicknesses of about 190, 28, and 9 ft. All curves are dissymmetrical. In the cases of the 190- and 28-ft beds, note the comparatively low readings in the upper 19 ft of the resistive bed and the high resistivity readings near the lower boundary. For the 190-ft bed, the curve presents a fairly long plateau with readings about equal to R_t; a minimum bed thickness of about 50 ft is needed to obtain these plateau readings uninfluenced by surrounding formations. In the case of the thin bed, there is a fairly sharp resistivity peak opposite the bed, followed by low readings over the "blind zone" below the bed, then a spurious "reflection" peak equal to the AO spacing below the bed. The relationship shown on the figure $(R_{amax}/R_{amin}) \leq (R_t/R_s)$ is of interest, even if accuracy of bed R_t cannot be expected.

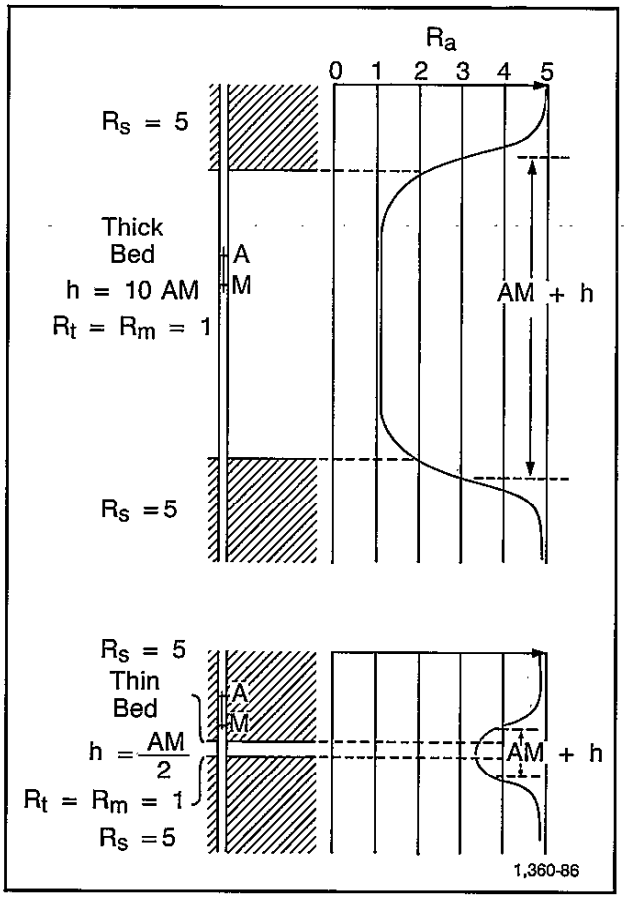

Fig. 7-4—Normal curves—bed less resistive than adjacent formations.

Fig. 7-6 illustrates the response of the lateral device in beds less resistive than the surrounding formations. The curves are again dissymmetrical. In both cases, the anomaly extends below the bed for a distance slightly greater than the AO spacing.

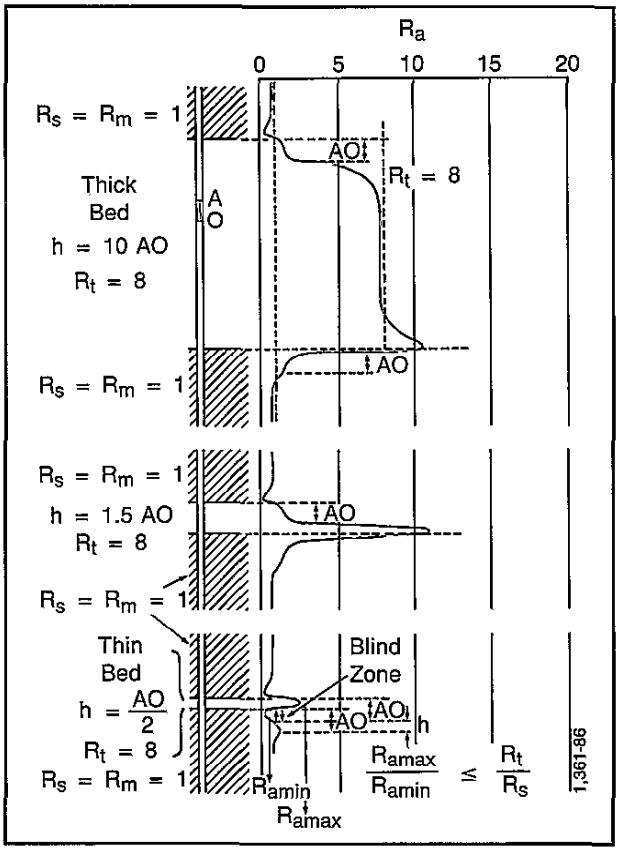

Fig. 7-5—Lateral curves—bed more resistive than adjacent formations.

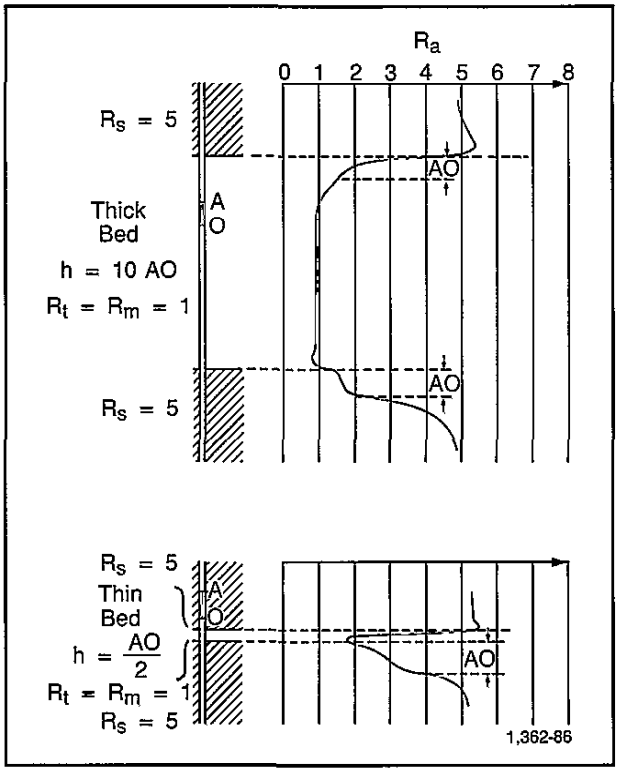

Fig. 7-6—Lateral curves—bed less resistive than adjacent formations.

Figs. 7-3 through 7-6 correspond to formations having moderate resistivities. In highly resistive formations, the normal curves are no longer symmetrical. Fig. 7-7 illustrates a thick bed of infinite resistivity. A two-electrode normal device would still give a symmetrical curve (dash-dot trace), but a three-electrode normal device, as was actually employed, gives a triangular-shaped curve (solid trace) with the peak of the triangle located at a distance AN below the upper boundary. The lateral curve also has a triangular shape, with the peak opposite the lower boundary. Also note that the lateral curve reads very low in the upper 19 ft of the bed.

If the borehole is bottomed in a thick formation of infinite resistivity, the lateral curve reads zero and the normal device gives a constant reading as long as the N electrode remains in the resistive bed (Fig. 7-8). The shapes of the normal and lateral curves become very complicated in highly resistive formations.

R_t From the ES Log

General rules for obtaining R_t from electrical logs are based on the relative resistivity of the bed compared to the resistivities of the mud and surrounding formation. Therefore, formations are subdivided into three classes, depending on the ratio $R_{16''}/R_m$. These simplifying rules are derived from a study of resistivity departure curves.

1. Low Resistivity—when $R_{16''}/R_m < 10$ (invasion up to $2d$)

   The shorter spacings, such as 16- and 64-in. normals, are most useful in finding R_t. Often, $R_m \cong R_s$, in which case the apparent value of the 64-in. normal can be easily corrected to R_t, depending on the ratio $R_{64''}/R_s$ and the bed thickness (see Fig. 7-9).

2. Medium Resistivity—when $10 < R_{16''}/R_m < 50$

   In this case, the 64-in. normal is very useful in the lower portion of the resistivity range; when $R_{16''}/R_m > 20$, the 18-ft 8-in. lateral becomes important, either to find R_t or to confirm the apparent 64-in. normal value. The lateral has an unsymmetrical curve, and R_t must be picked as shown in Fig. 7-9.

3. High Resistivity—when $R_{16''}/R_m > 50$

   The 64-in. normal is greatly affected by invasion so the 18-ft 8-in. lateral is the best choice for estimating R_t.

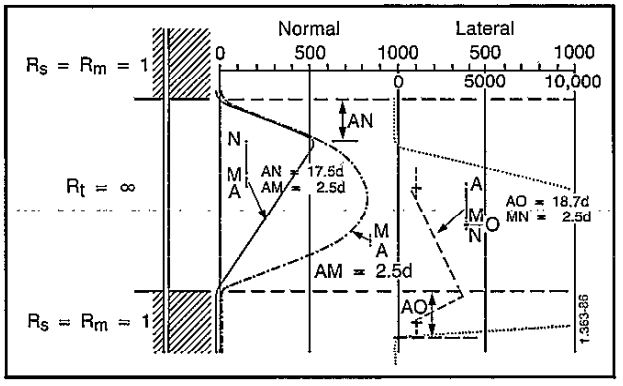

Fig. 7-7—Two-electrode and three-electrode normals and lateral curves in thick bed of infinite resistivity.

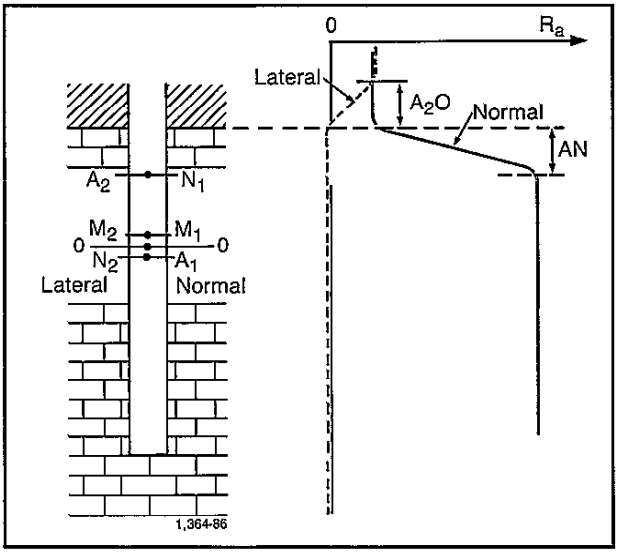

Fig. 7-8—Normal and lateral curves in highly resistive bed incompletely penetrated by borehole.

FOCUSING ELECTRODE LOGS

The responses of conventional electrical logging systems can be greatly affected by the borehole and adjacent formations. These influences are minimized by a family of resistivity tools that uses focusing currents to control the path taken by the measure current. These currents are emitted from special electrodes on the sondes.

The focusing electrode tools include the laterolog and SFL* spherically focused devices. These tools are much superior to the ES devices for large R_t/R_m values (salt muds and/or highly resistive formations) and for large resistivity contrasts with adjacent beds (R_t/R_s or R_s/R_t). They are also better for resolution of thin to moderately thick beds. Focusing electrode systems are available with deep, medium, and shallow depths of investigation.

Devices using this principle have as quantitative applications the determination of R_t and R_{xo}. The deep-reading devices include the Laterolog 7, the Laterolog 3, and the deep laterolog of the DLL* dual laterolog tool. The medium- to shallow-reading devices, all integral with combination tools, are the Laterolog 8 of the DIL* dual induction-laterolog tool, the shallow laterolog of the DLL tool, and the SFL of the ISF and DIL-SFL combinations.

Laterologs 3, 7, and 8 are now obsolete but their design principles will be discussed since many wells have been logged with these devices over the years.

Laterolog 7

The LL7 device comprises a center electrode, A_O, and three pairs of electrodes: M_1 and M_2; M'_1 and M'_2; and A_1 and A_2 (Fig. 7-10). The electrodes of each pair are symmetrically located with respect to A_O and are electrically connected to each other by short-circuiting wire.

A constant current, i_o, is emitted from A_O. Through bucking electrodes, A_1 and A_2, an adjustable current is emitted; the bucking current intensity is adjusted automatically so that the two pairs of monitoring electrodes, M_1 and M_2 and M'_1 and M'_2, are brought to the same potential. The potential drop is measured between one of the monitoring electrodes and an electrode at the surface (i.e., at infinity). With a constant i_o current, this potential varies directly with formation resistivity.

Since the potential difference between the M_1-M_2 pair and the M'_1-M'_2 pair is maintained at zero, no current from A_O is flowing in the hole between M_1 and M'_1 or between M_2 and M'_2. Therefore, the current from A_O must penetrate horizontally into the formations.

Fig. 7-10 shows the distribution of current lines when the sonde is in a homogeneous medium; the "sheet" of i_o current retains a fairly constant thickness up to a distance from the borehole somewhat greater than the total length A_1A_2 of the sonde. Experiments have shown that the sheet of i_o current retains substantially the same shape opposite thin resistive beds.

The thickness of the i_o current sheet is approximately 32 in. (distance O_1O_2 on Fig. 7-10), and the length A_1A_2 of the sonde is 80 in.

Fig. 7-11 compares the curves obtained experimentally opposite a thin resistive bed using the conventional devices (16-in. and 64-in. normals and 18-ft 8-in. lateral) with the corresponding LL7 recording. The conventional devices give poor results; the LL7 curve, in spite of difficult conditions (R_t/R_m is 5000), shows the bed very clearly and reads close to R_t.

Laterolog 3

The LL3 tool also uses currents from bucking electrodes to focus the measuring current into a horizontal sheet

* Mark of Schlumberger

Bed Thickness (e)	Qualifications	Device	Response
A. In low resistivity, when $R_{16''}/R_m < 10$ (invasion up to 2d)			
e > 20 ft (> 4 AM′)		Long Normal	$R_{64''} = R_t$
e ≅ 15 ft (3 AM′)	$R_m \cong R_s$ $R_{64''}/R_s \geq 2.5$	Long Normal	$R_{64''} = \frac{2}{3} R_t$
e ≅ 15 ft (3 AM′)	$R_m \cong R_s$ $R_{64''}/R_s \leq 1.5$	Long Normal	$R_{64''} = R_t$
e ≅ 10 ft (2 AM′)	$R_m \cong R_s$ $R_{64''}/R_s \geq 2.5$	Long Normal	$R_{64''} = \frac{1}{2} R_t$
e ≅ 10 ft (2 AM′)	$R_m \cong R_s$ $R_{64''}/R_s = 1.5$	Long Normal	$R_{64''} = \frac{2}{3} R_t$
5 ft < e < 10 ft	When oil bearing and SP is −50 to −80 mV	Short Normal	$R_{16''} \cong R_t$
5 ft < e < 10 ft	Surrounding beds homogeneous	Lateral in resistive bed	$R_t \geq R_{max} \times R_s/R_{min}$
Thin beds (in general)	Surrounding beds homogeneous	Lateral in conductive bed	$R_{19''} \cong R_t$

B. Rules for using lateral (AO = 18 ft 8 in.)

e > 40 ft (> 2 AO)

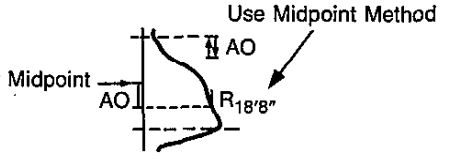

e ≅ 28 ft (= 1.5 AO)

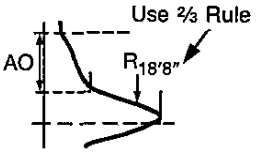

e ≅ 24 ft (= 1.3 AO)

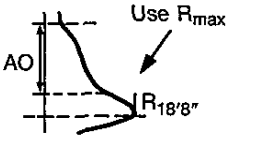

5 ft < e < 10 ft — Resistive bed and surrounding beds homogeneous

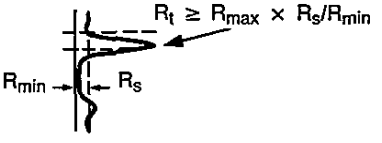

When $R_{16''}/R_m > 50$, these values must be corrected for the borehole: Chart B-2.

C. Response of Laterolog 7

e > 3 ft

For $d_i = 20$ in., $R_{LL} \cong 0.2\ R_{xo} + 0.8\ R_t$

For $d_i = 40$ in., $R_{LL} \cong 0.4\ R_{xo} + 0.6\ R_t$

For $d_i = 80$ in., $R_{LL} \cong 0.6\ R_{xo} + 0.4\ R_t$

Thus, the best results occur when $R_{xo} < R_t$ and $R_{mf}/R_w < 4$.

1,370-86

Fig. 7-9—R_t estimation from electrical logs.

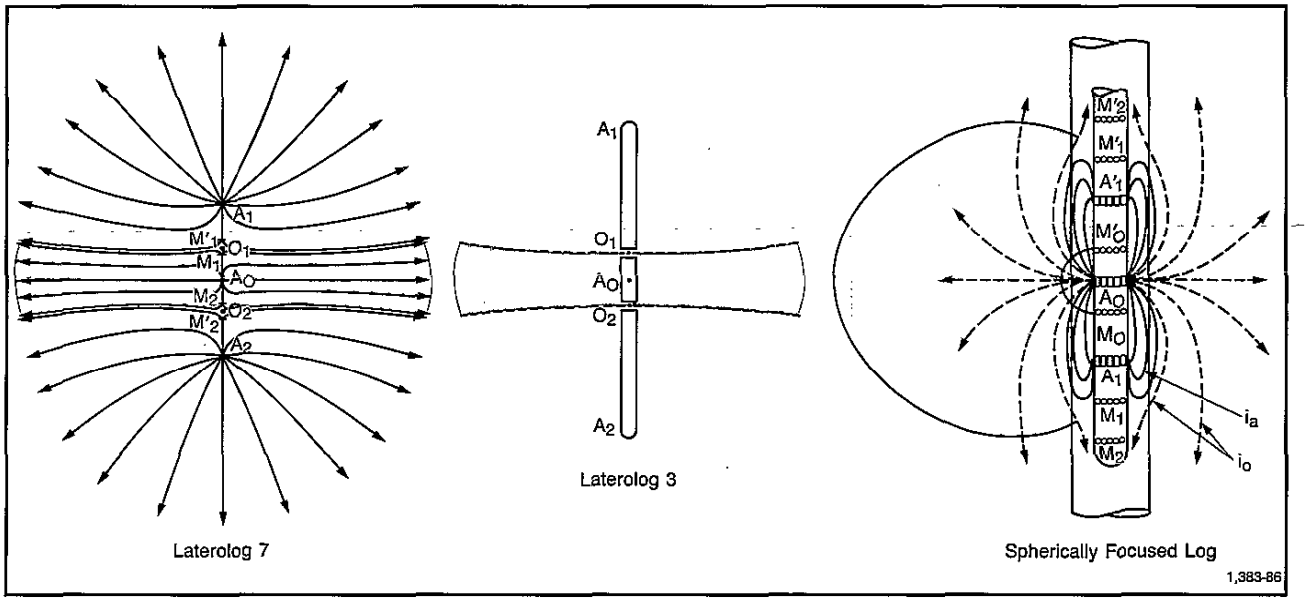

Fig. 7-10—Schematics of focusing electrode devices.

penetrating into the formation (Fig 7-10). Symmetrically placed on either side of the central A_O electrode are two very long (about 5-ft) electrodes, A_1 and A_2, which are shorted to each other. A current, i_o, flows from the A_O electrode, whose potential is fixed. From A_1 and A_2 flows a bucking current, which is automatically adjusted to maintain A_1 and A_2 at the potential of A_O. All electrodes of the sonde are thus held at the same constant potential. The magnitude of the i_o current is then proportional to formation conductivity.

The i_o current sheet is constrained to the disk-shaped area. The thickness, O_1O_2, of the current sheet is usually about 12 in., much thinner than for the LL7 device. As a result, the LL3 tool had a better vertical resolution and shows more detail than did the LL7 tool. Furthermore, the influences of the borehole and of the invaded zone were slightly less.

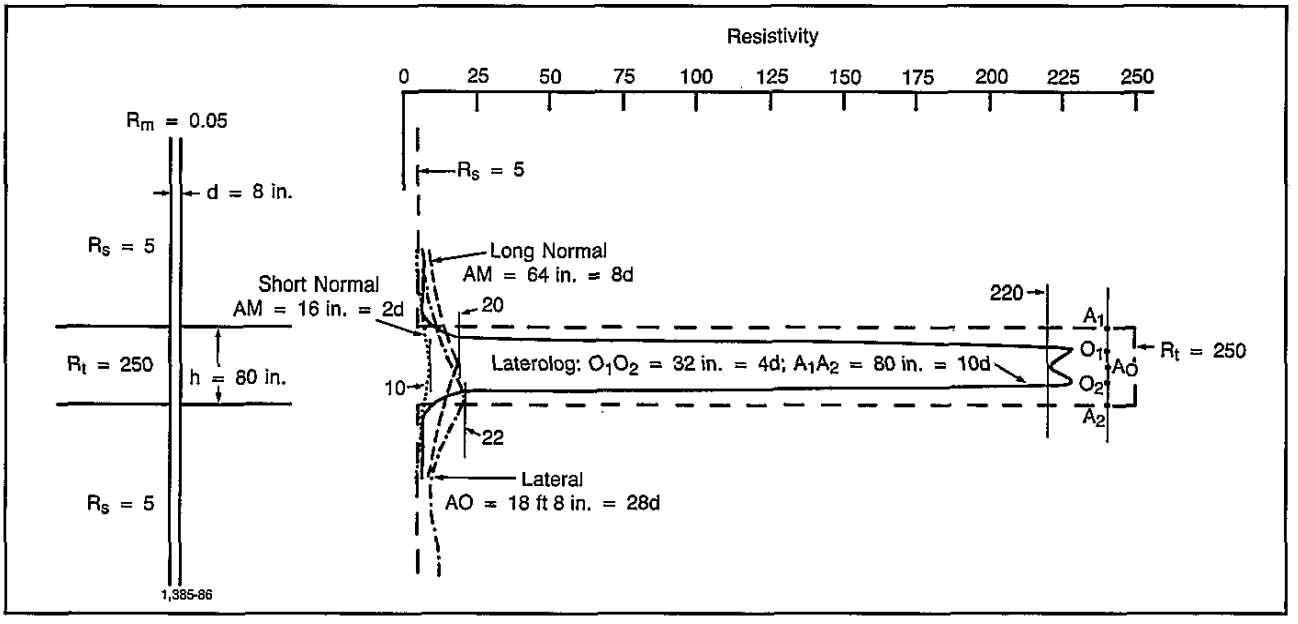

Fig. 7-11—Response of Laterolog 7 and ES opposite a thin, resistive, noninvaded bed with very salty mud (laboratory determinations).

Laterolog 8

The shallow-investigation LL8 measurement is recorded with small electrodes on the dual induction-laterolog sonde. The device is similar in principle to the LL7 tool except for its shorter spacings. The thickness of the i_0 current sheet is 14 in., and the distance between the two bucking electrodes is somewhat less than 40 in. The current-return electrode is located a relatively short distance from A_O. With this configuration, the LL8 device gives sharp vertical detail, and the readings are more influenced by the borehole and the invaded zone than are those of the LL7 and LL3 tools.

Dual Laterolog-R_{xo} System

The objective of any deep-reading resistivity device is to measure the true formation resistivity, R_t. Deep-reading resistivity tools were designed so that, as much as possible, their response is determined by the resistivity of the virgin formation beyond the invaded zone. Unfortunately, no single measurement has yet succeeded in entirely eliminating the effects of the invaded zone.

A solution is to measure the resistivity with several arrays having different depths of investigation. Measurements responding to three appropriately chosen depths of investigation usually approximate the invasion profile well enough to determine R_t.

For best interpretation accuracy such a combination system should have certain desirable features:

- Borehole effects should be small and/or correctable.
- Vertical resolutions of the devices should be similar.
- Radial investigations should be well distributed; i.e., one reading as deep as practical, one reading very shallow, and the third reading in between.

This need resulted in the development of the DLL dual laterolog-MicroSFL tool with simultaneous recordings. Fig. 7-12 is a sketch of the tool showing the electrode array used for the two laterolog devices. Both use the same electrodes and have the same current-beam thickness, but have different focusing to provide their different depth of investigation characteristics. Fig. 7-13 illustrates the focusing used by the deep laterolog device (left) and by the shallow laterolog device (right).

The DLL tool has a response range of 0.2 to 40,000 ohm-m, which is a much wider range than covered by previous laterolog devices.

To achieve accuracy at both high and low resistivities, a "constant-power" measuring system is employed. In this system, both measure current (i_0) and measure voltage (V_0) are varied and measured, but the product of the two (i.e., power), i_0V_0, is held constant.

The deep laterolog measurement (LLD) of the DLL tool has a deeper depth of investigation than previous

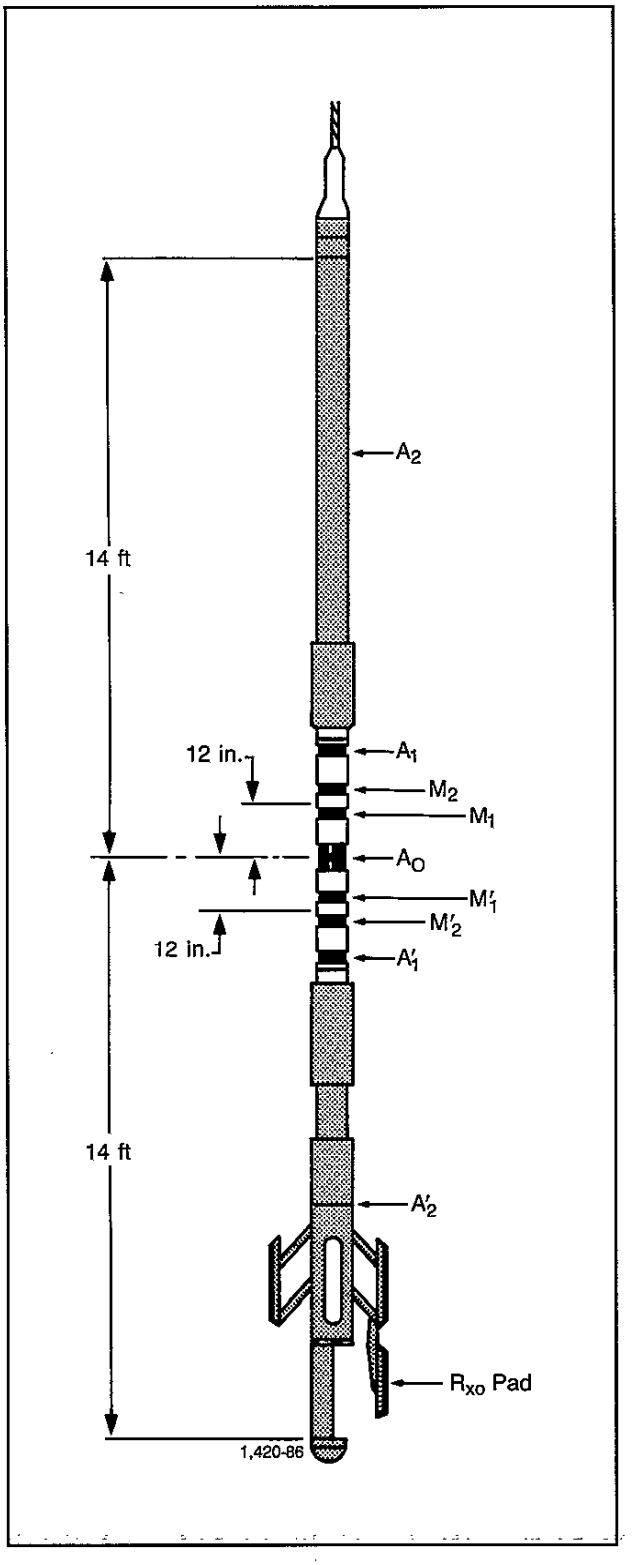

Fig. 7-12—Schematic diagram of the Dual Laterolog-R_{xo} tool.

laterolog tools and extends the range of formation conditions in which reliable determinations of R_t are possible.

To achieve this, very long guard electrodes are needed; the distance between the extreme ends of the guard electrodes of the DLL-R_{xo} tool is approximately 28 ft. The nominal beam thickness of 2 ft, however, insures good vertical resolution.

The shallow laterolog measurement (LLS) has the same vertical resolution as the deep laterolog device (2 ft), but it responds more strongly to that region around the borehole normally affected by invasion. It uses a type of focusing called "pseudolaterolog," wherein the focusing current is returned to nearby electrodes instead of to a remote electrode. This causes the measure current to diverge more quickly once it has entered the formations, thus producing a relatively shallow depth of investigation.

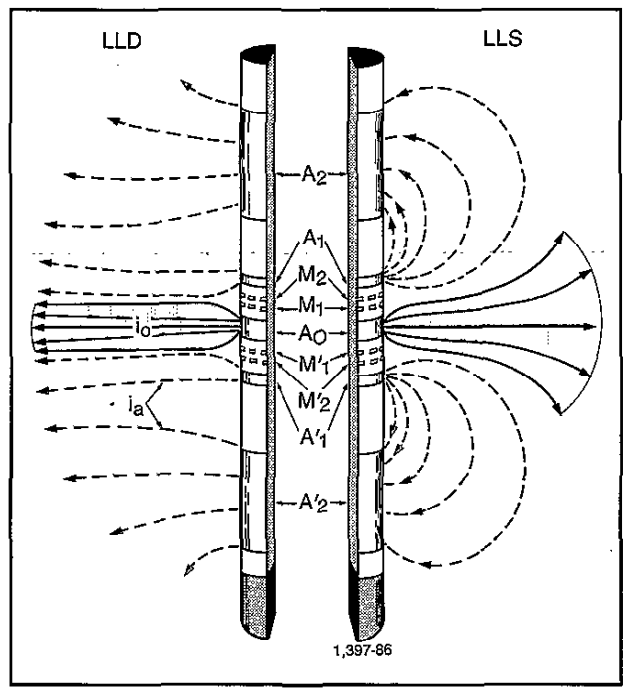

Fig. 7-13—Schematic of the Dual Laterolog.

Delaware Effect

If both B and N electrodes are placed downhole, LLD readings may exhibit a "Delaware effect" (or gradient) in sections located just below thick nonconductive beds such as anhydrite. It appears as abnormally high resistivity for about 80 ft below the resistive bed.

Fig. 7-14 illustrates the effect and its cause. As B electrode enters the thick anhydrite, the current flow is confined to the borehole, and if the bed is thick enough (several hundred feet) practically all the current will flow in that part of the borehole below B. Then when N electrode enters the bed, it can no longer remain at zero potential as intended. It is exposed to an increasing negative potential as it rises farther from the bed boundary. This potential causes a gradual increase (gradient) in the recorded resistivity.

The LLD device uses surface electrodes for current return so it is not subject to Delaware effect. However, a small anti-Delaware effect has been observed that produces resistivities that are slightly low immediately below the resistive bed. This problem was minimized by using cable armor as the reference electrode for the measure potential.

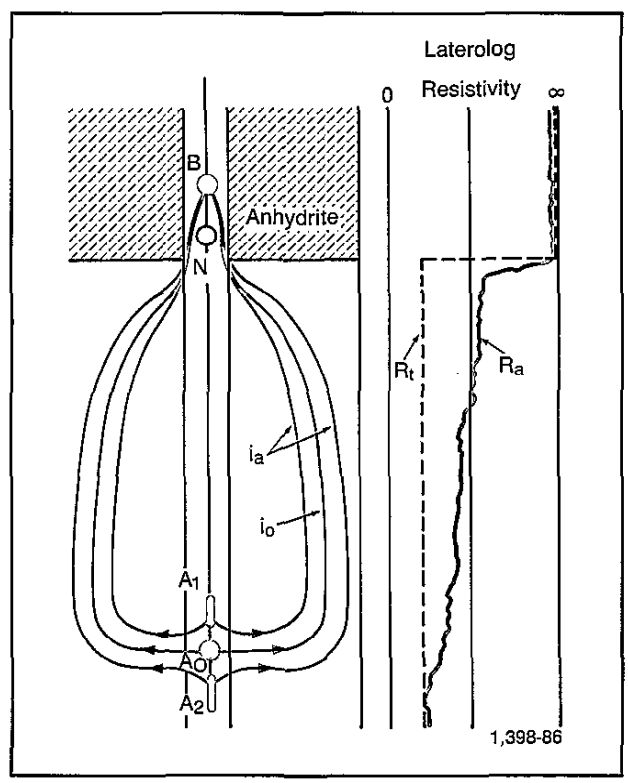

Fig. 7-14—Principle of Delaware effect.

Groningen Effect

An effect similar to the Delaware gradient was later noticed on the LLD curve. It is called the "Groningen" effect, after the large Dutch gas field where the anomaly was first discovered. The Groningen effect occurs for about 100 ft below a thick, highly resistive bed. Since the measure and bucking current cannot flow easily through the highly resistive bed, it returns through the mud column and creates a negative potential on the "zero reference electrode." If casing has been set in the resistive zone, it helps to "short circuit" the current and the Gron-

ingen effect is even more pronounced. An induction log is recommended for serious formation evaluation in these "shielded" conductive beds.

Scales

A problem common to all resistivity and conductivity devices is providing a scale that can be read accurately over the full range of response. Years ago, most laterologs were recorded on linear scales. Because of the very large range of resistivities often encountered, the required scale was relatively insensitive. Very low readings, whether resistivity or conductivity, were virtually unreadable. Backup curves of increased sensitivity were introduced, but they were difficult to read and cluttered the log in formations of high contrast.

For a while, the hybrid scale, first used on the LL3 tool, was employed. It presented linear resistivity over the first half of the grid track (log), and linear conductivity over the last half. Thus, one galvanometer could record all resistivities from zero to infinity. Although somewhat awkward to use because of the odd scale divisions (see Fig. 7-15a), the hybrid scale did provide acceptable sensitivity in both low-resistivity and low-conductivity formations.

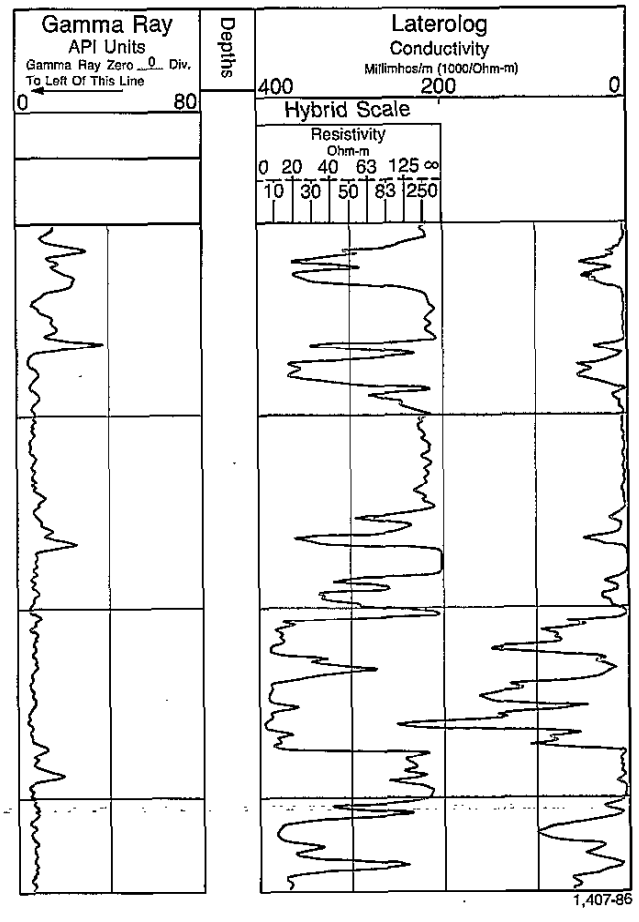

Fig. 7-15a—Laterolog recorded on hybrid scale.

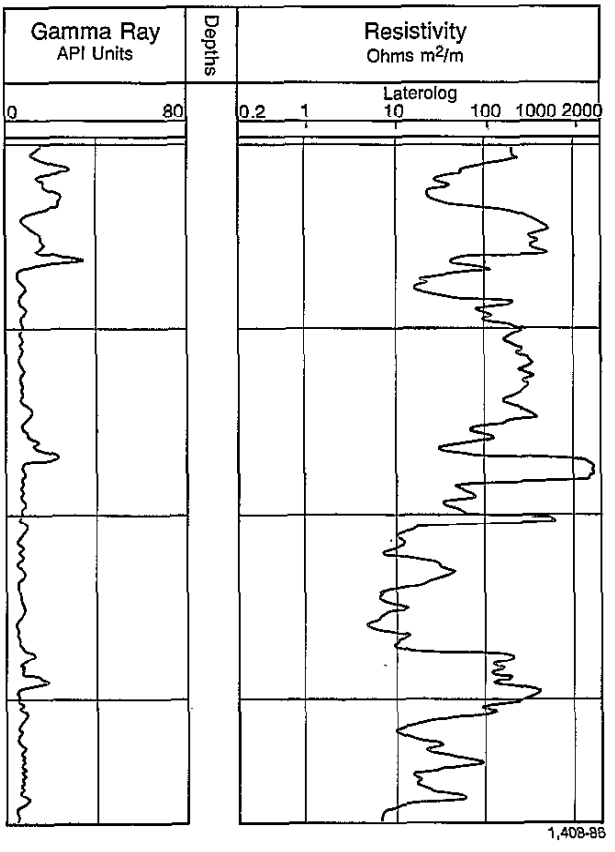

Fig. 7-15b—Laterolog over same interval as in Fig. 7-15a recorded on logarithmic scale.

Today, the logarithmic scale is the most acceptable scale for recording resistivity curves. Its standard form is a split four-cycle grid covering the range from 0.2 to 2000 ohm-m (see Fig. 7-15b). Even this range is sometimes not sufficient for the DLL-R_{xo} measurements; when needed, a backup trace is used to cover the range from 2000 to 40,000 ohm-m.

Spherically Focused Log

The SFL device measures the conductivity of the formation near the borehole and provides the relatively shallow investigation required to evaluate the effects of invasion on deeper resistivity measurements. It is the short-spacing device now used on the DIL-SFL tool—developed to replace the 16-in. normal and LL8 devices.

The SFL system differs from previous focused electrode devices. Whereas the LL7 and LL8 systems attempt to focus the current into planar discs, the SFL system establishes essentially constant potential shells around the current electrode. The SFL device is able to preserve the spherical potential distribution in the formation over a wide range of wellbore variables, even when a conduc-

tive borehole is present. To accomplish this, the SFL device is composed of two separate, and more or less independent, current systems. The bucking current system serves to "plug" the borehole and establish the equipotential spheres. The i_0 survey current system causes an independent survey current to flow through the "volume of investigation"; the intensity of this current is proportional to formation conductivity.

The SFL device consists of current-emitting electrodes, current-return electrodes, and measure electrodes. Two equipotential spheres about the tool's current source are established. The first sphere is about 9 in. away from the survey current electrode; the other is about 50 in. away. A constant potential of 2.5 mV is maintained between these two spherical surfaces. Since the volume of formation between these two surfaces is constant (electrode spacing is fixed) and the voltage drop is constant (2.5 mV), the conductivity of this volume of formation can be determined by measuring the current flow.

Influence of Wellbore Variables and Log Corrections

The laterolog and SFL readings, like most resistivity measurements, are influenced by the borehole mud, the adjacent (shoulder) beds, and the invaded zone. Charts have been constructed from a series of mathematical simulations to correct the log readings for these influences. The corrections must always be made in this order—borehole, bed thickness, invasion.

Borehole Effect

Charts Rcor-2a and -2b are borehole-correction charts for deep and shallow laterolog readings for a centered sonde. Eccentering has little effect on the LLD curve, but it can be detrimental to the LLS reading when the ratio R_t/R_m is high. Chart Rcor-2c is for eccentered sondes. Chart Rcor-1 provides borehole corrections for the LL8 and SFL devices employed on the DIL-LL8 and DIL-SFL tools. Chart Rcor-3 corrects the SFL device used on the Phasor induction tool for borehole effects.

Adjacent Bed Effect

Chart Rcor-8 gives the shoulder bed-effect corrections needed for the deep and shallow laterolog readings of the DLL tool in noninvaded beds with infinitely thick shoulder beds of similar resistivity.

Readings must be corrected for borehole effect before the shoulder-bed charts are entered. Fig. 7-16 provides bed-thickness corrections for the LL3 and LL7 measurements.

Pseudogeometrical Factors

Geometrical factor can be defined as that fraction of the total signal that would originate from a volume having a specific geometrical orientation with the sonde in an infinite homogeneous medium. The only logging devices for which this concept is reasonably rigorous are the induction tools. However, for comparative evaluations, it is useful to construct charts based on pseudogeometrical factors for other resistivity devices. Such a chart is shown in Fig. 7-17, where the integrated pseudogeometrical factors of progressively larger cylinders are plotted versus the diameters of the cylinders. The apparent resistivity, R_a, measured in a thick bed is given approximately by

$$R_a = J(d_i)\, R_{xo} + [1 - J(d_i)]\, R_t, \quad \text{(Eq. 7-3)}$$

where $J(d_i)$ is the pseudogeometrical factor. A pseudogeometrical factor relating to an electrode-type resistivity device is applicable in only one set of conditions; therefore, charts of this type are not valid as general-purpose invaded-zone correction charts. The most useful feature of this chart is its graphic comparison of the relative contribution of the invaded zone to the responses of the various tools and, therefore, of the relative depths of investigation of the individual tools.

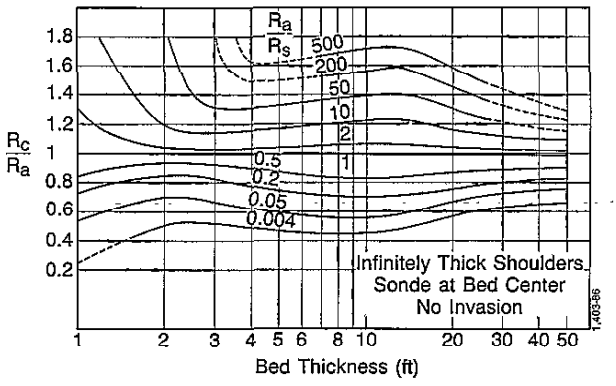

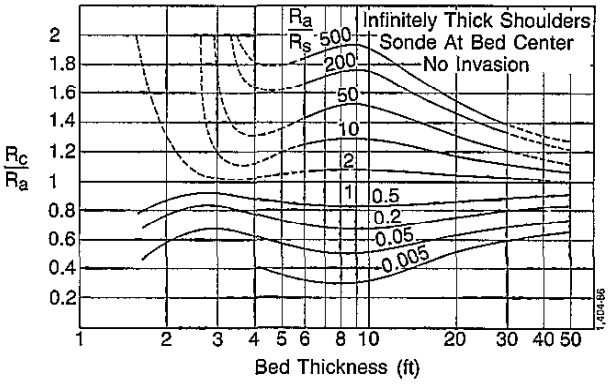

Fig. 7-16b—Shoulder-bed correction, Laterolog 7.

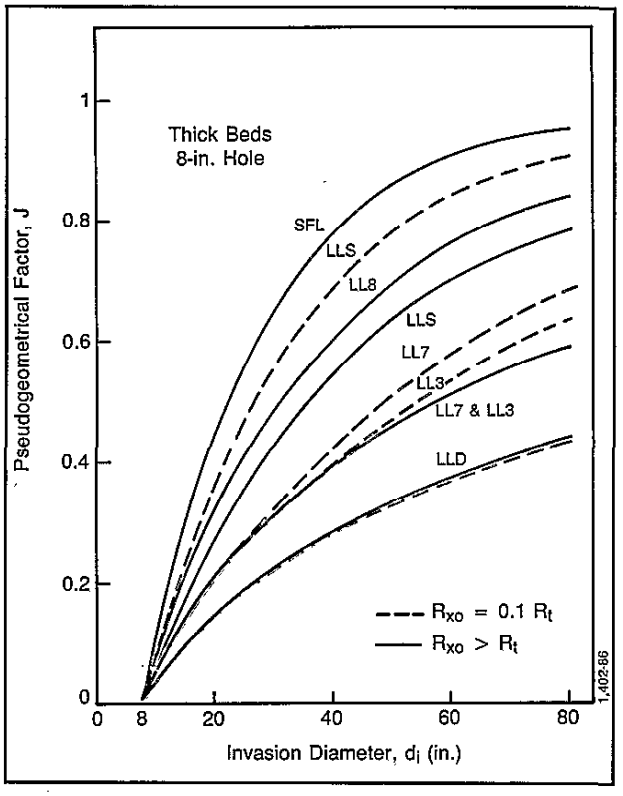

Fig. 7-17—Radial pseudogeometrical factors, fresh muds (solid) and salty muds (dashed).

Note the excellent spread in radial characteristics of the deep and shallow laterolog measurements. This feature permits accurate resistivity analysis over a wide range of invasion conditions.

Invasion Correction

Eq. 7-3 contains three unknowns: the flushed zone resistivity, R_{xo}; the true resistivity of the virgin, uncontaminated zone, R_t; and the diameter of invasion, d_i. If a step profile of invasion is assumed, a combination of deep and shallow laterolog measurements with a very shallow R_{xo} resistivity measurement, such as the MicroSFL or microlaterolog, can be used to solve for the three unknowns.

Chart Rint-9 performs this solution graphically. The true resistivity value obtained can be used in the Archie water saturation equation to determine saturation, or the R_{xo}/R_t resistivity ratio can be used for the same purpose in the ratio water saturation equation.

INDUCTION LOGGING

The induction logging tool was originally developed to measure formation resistivity in boreholes containing oil-base muds and in air-drilled boreholes. Electrode devices did not work in these nonconductive muds, and attempts to use wall-scratcher electrodes were unsatisfactory.

Experience soon demonstrated that the induction log had many advantages over the conventional ES log when used for logging wells drilled with water-base muds. Designed for deep investigation, induction logs can be focused in order to minimize the influences of the borehole, the surrounding formations, and the invaded zone.

Principle

Today's induction tools have many transmitter and receiver coils. However, the principle can be understood by considering a sonde with only one transmitter coil and one receiver coil (Fig. 7-18).

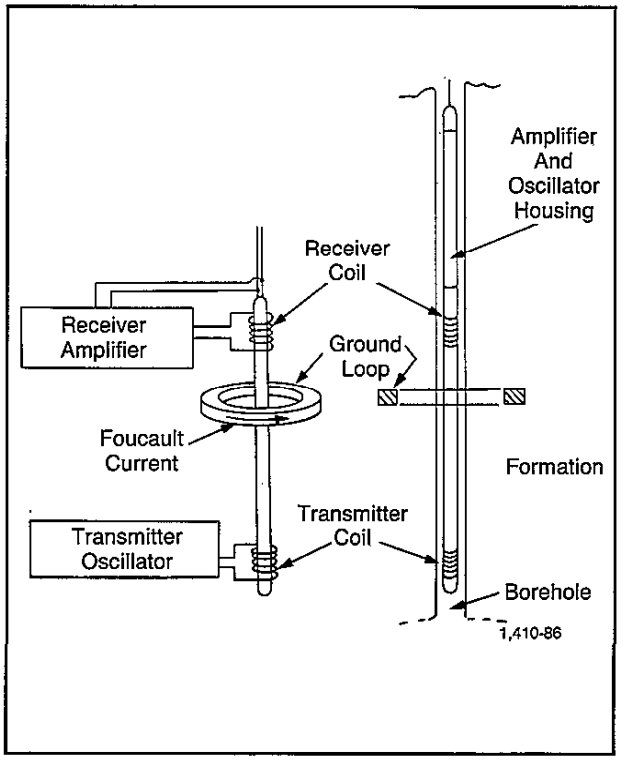

Fig. 7-18—Basic two-coil induction log system.

A high-frequency alternating current of constant intensity is sent through a transmitter coil. The alternating magnetic field created induces currents in the formation surrounding the borehole. These currents flow in circular ground loops coaxial with the transmitter coil and create, in turn, a magnetic field that induces a voltage in the receiver coil.

Because the alternating current in the transmitter coil is of constant frequency and amplitude, the ground loop

currents are directly proportional to the formation conductivity. The voltage induced in the receiver coil is proportional to the ground loop currents and, therefore, to the conductivity of the formation.

There is also a direct coupling between the transmitter and receiver coils. The signal originating from this coupling is eliminated by using "bucking" coils.

The induction tool works best when the borehole fluid is an insulator—even air or gas. The tool also works well when the borehole contains conductive mud unless the mud is too salty, the formations are too resistive, or the borehole diameter is too large.

Geometrical Factor

If the model is simplified (sonde centered and formation homogeneous and isotropic), the tool response can be calculated as the sum of the elementary signals created by all formation loops coaxial with the sonde. This neglects the mutual and self-inductance of the ground loops. Each elementary signal is proportional to the loop conductivity and to a geometrical factor that is a function of the loop position with reference to the transmitter and receiver coils. Therefore,

$$E = K \Sigma g_i C_i, \qquad \text{(Eq. 7-4)}$$

where

E is the induced electromotive force,

K is the sonde constant,

g is the geometrical factor for that particular loop,

C is the conductivity of that loop,

and

$\Sigma g_i = 1$.

The geometrical factor, g_i, corresponding to a medium is defined as the proportion of the total conductivity signal contributed by the given medium. As shown in Chart Gen-3, the formation can be split into cylinders coaxial with the sonde (tool being centralized); they correspond to the mud column, invaded zone, virgin zone, and shoulder beds. The total signal can be expressed by

$$C_I = G_m C_m + G_{xo} C_{xo} + G_t C_t + G_s C_s, \qquad \text{(Eq. 7-5)}$$

where

$$G_m + G_{xo} + G_t + G_s = 1$$

and where G is the geometrical factor for a defined region.

Thus, a volume of space defined only by its geometry relative to the sonde has a fixed and computable geometrical factor (G) (see Fig. 7-19). This permits the construction of mathematically sound correction charts to account for the effects of borehole mud, invaded zone, and adjacent beds on the R_t measurement, providing symmetry of resolution exists.

Because induction tools are designed to evaluate R_t, it is important to minimize terms relative to the mud, the invaded zone, and the shoulder beds. This is done by minimizing the corresponding geometrical factors with a focused signal.

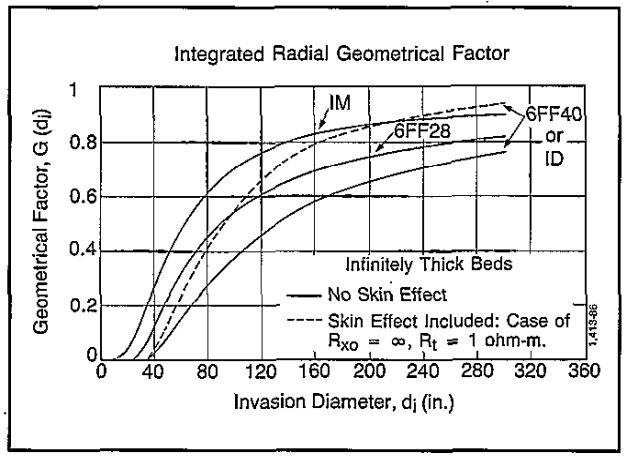

Fig. 7-19—Geometrical factors. Dashed curve includes skin effect, under conditions shown, for the 6FF40 or the deep induction (ID) devices.

Focusing

The simple two-coil system does not represent the tool used today. However, it can be considered the building block from which today's multicoil sonde was built. The response of a multicoil sonde is obtained by breaking it down into all possible two-coil combinations of transmitter-receiver pairs. The response of each coil pair is weighted by the product of the number of turns on the two coils and by the product of their cross-sectional area. The responses of all coil pairs are added, with due regard to the algebraic sign of their contributions and their relative positions.

Multicoil sondes, or focused sondes, offer certain advantages. Vertical resolution is improved by suppressing the response from the shoulder formations, and depth of investigation is improved by suppressing the response from the mud column and the formation close to the hole.

Deconvolution

Deconvolution is the extraction of desirable components of a complex signal by variously weighting the gross measurement at different points relative to the objective zone. Deep induction measurements are made possible,

without sacrificing vertical resolution, by a deconvolution that gives greater proportional weight to the signal measured at the sonde center than to signals measured above and below that point.

In the past, various weighted deconvolutions were used to account for differing values of shoulder-bed resistivity, but this practice has been abandoned in the interest of standardization. Most of today's logs are run with shoulder-bed resistivity settings of 1 ohm-m, and deconvolution is performed by the CSU* surface equipment software. Deconvolution is done before skin-effect boost is applied.

Skin Effect

In very conductive formations the induced secondary currents in the ground loops are large, and their magnetic fields are important. The magnetic fields of these ground loops induce additional emf's (electrical voltages) in other ground loops. These induced emf's are out of phase with those induced by the transmitter coil of the induction tool. This interaction between the ground loops causes a reduction of the conductivity signal recorded on the induction logs, which is called "skin effect." It is a predictable phenomenon. Fig. 7-20 shows the response of the tool compared to the actual formation conductivity of the formation. Skin effect becomes significant when formation conductivity exceeds 1,000 mmho/m.

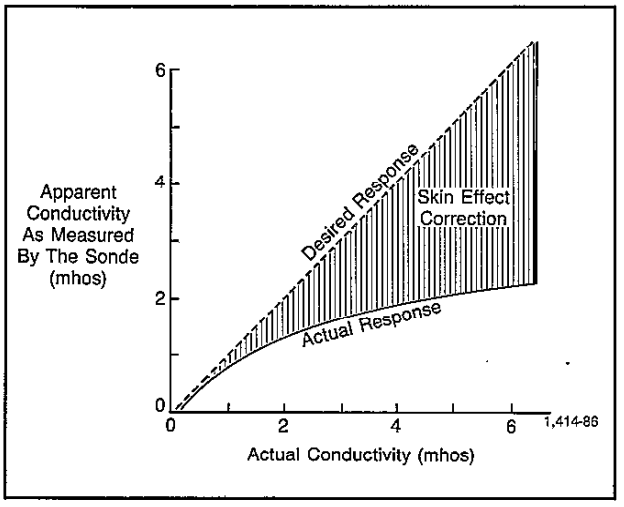

Fig. 7-20—Actual response of an induction log compared to the "desired" response.

Schlumberger induction logs are automatically corrected for skin effect during recording. The correction is based on the magnitude of the uncorrected tool response, treated as if it were from a homogeneous medium. A secondary skin-effect correction may be required when the media surrounding the sonde are not of uniform conductivity. These corrections are usually incorporated in the various interpretation charts that involve induction logs.

Equipment

The induction tool has been the basic resistivity tool used in logging low- to medium-resistivity formations drilled with fresh water, oil, or air for over 25 years. During that period, several types of equipment have been developed and used.

1. The 6FF40 induction-electrical survey (IES) tool included a six-coil focused induction device of 40-in. nominal spacing (hence, the nomenclature, 6FF40), a 16-in. normal, and an SP electrode. The tool was first introduced in the late 1950's and was the standard induction tool throughout the 1960's. It has since been replaced by improved tools.
2. The DIL-LL8 system used a deep-reading induction device (the ID, which was similar to the 6FF40), a medium induction device (the IM), an LL8 device (which replaces the 16-in. normal), and an SP electrode.

   The IM device has a vertical resolution similar to that of the 6FF40 (and ID) but only about half the depth of investigation (see Fig. 7-19). The LL8 was a focused, shallow-investigation device with better thin-bed resolution and less borehole influence than the 16-in. normal. It was also void of some disturbing characteristics of normal devices—such as reversals in thin resistive beds.
3. The induction-SFL (ISF) tool incorporated a deep induction device similar to the 6FF40, the SFL device, and an SP electrode. The tool was combinable with the borehole compensated sonic tool and with a gamma ray (GR) device. The combination offered, in certain geological horizons, the ability to evaluate the hydrocarbon potential of the well in a single logging run. The sonic log provided porosity evaluation and the ISF log provided saturation evaluation.
4. The DIL-SFL tool is similar to the DIL-LL8 tool except that the SFL has replaced the LL8 as the shallow-investigation device. The SFL measurement is less influenced by the borehole than is the LL8 measurement (see Chart Rcor-1).
5. The Phasor* Induction SFL tool has a deep-reading induction device (IDPH), a medium-reading induction device (IMPH), an SFL device, and an SP electrode. The tool employs a digital transmission and processing system and a continuous calibration verification system. It also can be operated at frequencies of 10 and 40 kHz, as well as at 20 kHz (the operating frequency of most previous induction devices).

* Mark of Schlumberger

6. The 6FF28 IES tool (2⅝-in. diameter) is a scaled-down version of the 6FF40 device, having a 28-in. primary coil spacing, and includes a standard 16-in. normal device and an SP electrode. It is used for logging in small holes and for through-drillpipe operations.

Log Presentation and Scales

The SP and/or GR curves are recorded in Track 1 for all tools.

Fig. 7-21 illustrates the original IES presentation. The induction conductivity curve is sometimes recorded over both Tracks 2 and 3. The linear scale is in millimhos per meter (mmho/m), increasing to the left. In Track 2 both the 16-in. normal and the reciprocated induction curves are recorded on the conventional linear resistivity scale.

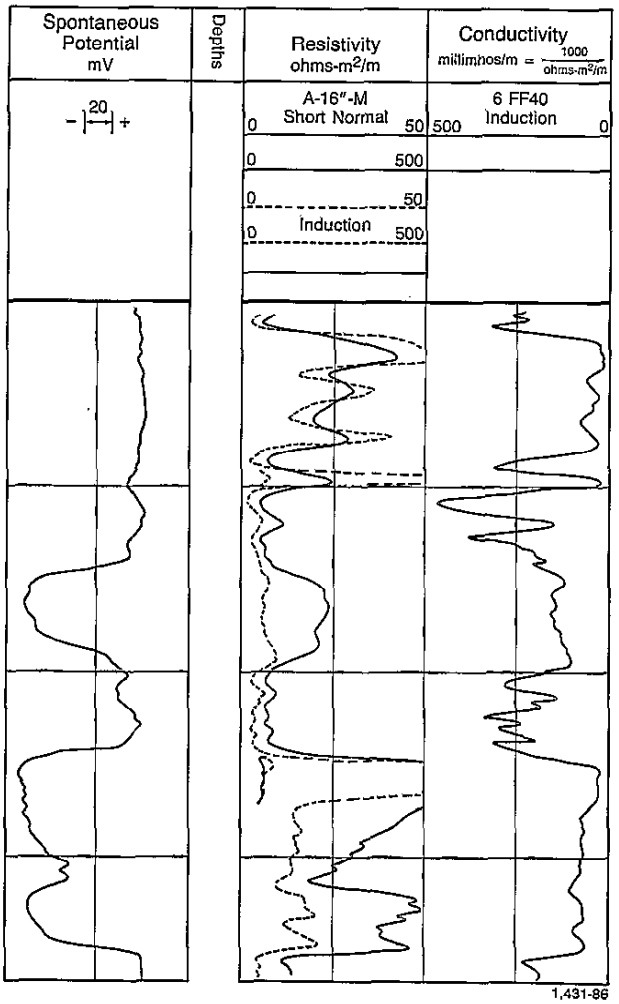

Fig. 7-21—Induction-electrical log presentation.

The DIL-LL8 log introduced the logarithmic grid; the standard presentation is shown in Fig. 7-22. Four decades of resistivity (usually 0.2 ohm-m to 2,000 ohm-m) were recorded over Tracks 2 and 3.

The DIL-SFL log, in combination with the sonic log, required a modification of this grid. Two decades of resistivity on logarithmic grid are presented in Track 2. The sonic transit time is presented in Track 3 on linear grid. The log presentation is shown in Fig. 7-23.

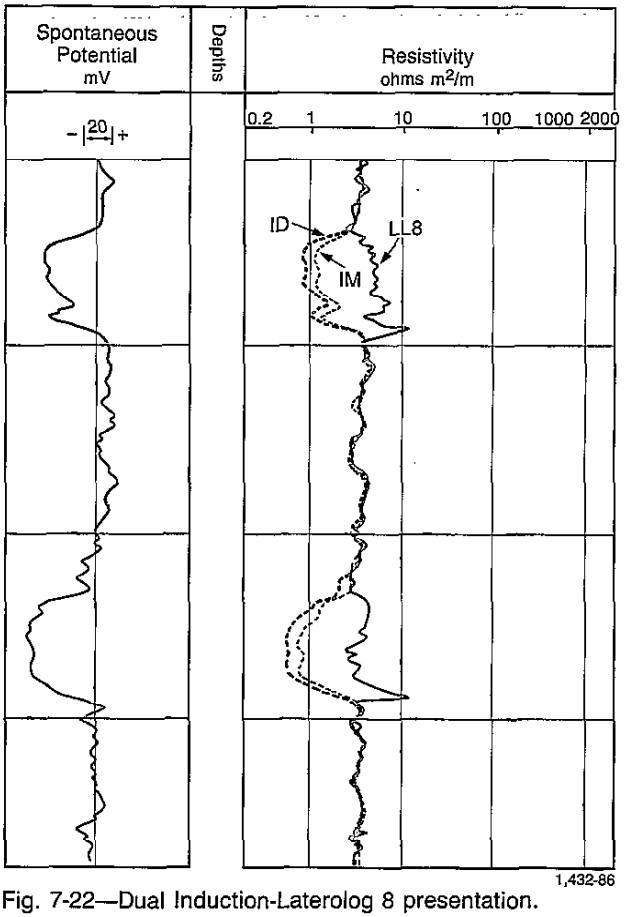

Fig. 7-22—Dual Induction-Laterolog 8 presentation.

Environmental Corrections Prior to Phasor Induction

As is true for all resistivity measurements, induction measurements may be influenced by the borehole, by surrounding beds, and by invasion. The induction log must be corrected for these effects before the measurements can be used. Since the induction logs have been specifically designed to minimize these effects, they are not normally large and can, in many situations, be ignored without major consequence. Nevertheless, it is wise to make these environmental corrections. There are three: a borehole correction, a surrounding bed correction, and an invasion correction. Charts are available to assist in making the corrections, and they must be made in the stated order: borehole, bed thickness, invasion.

Borehole Correction

Conductivity signals from the mud can be evaluated using geometrical factors. Chart Rcor-4 gives corrections for various curves (6FF40, ID, IM, 6FF28, IDPH, IMPH) and for various standoffs.

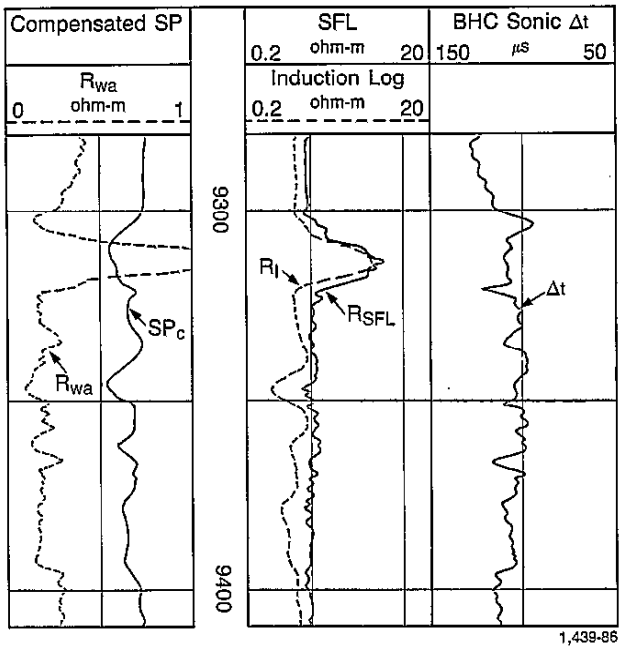

Fig. 7-23—ISF/sonic presentation.

The nominal borehole signal, based on bit size, is sometimes removed from the recorded log; when the hole signal is significant, consult the log heading to ascertain whether this was done. The precaution applies particularly to the medium induction devices because they are strongly influenced by borehole size.

Surrounding Bed Correction

Charts Rcor-5 and -6 provide bed-thickness corrections for the ID and IM, respectively. The need for a correction in thin beds is generally well recognized. Not so well recognized is the need for a correction when bed thickness is in the 10- to 30-ft range and bed resistivity exceeds 5 ohm-m.

The ID correction curves are valid for the 6FF40 measurement; these two induction devices are, for all practical purposes, identical. The ID correction curves are also valid for the 6FF28 provided the bed thickness is adjusted for the shorter coil spacing before entry into the chart.

To correct the ID (and 6FF40 and 6FF28) in thin conductive beds, Chart Rcor-7 is used. Chart Rcor-9 provides bed-thickness corrections for the Phasor induction measurements. The charts reflect the much superior bed-thickness response of the Phasor tool. For beds thicker than 6 ft, little or no surrounding bed correction is required.

Invasion Correction

The invasion correction charts are derived from geometrical factor considerations. If a step profile of invasion is assumed (a step profile is one in which the invading mud filtrate pushes all the connate water before it in a piston-like process), the responses of, say, the DIL-SFL measurements are as follows:

$$C_{ID} = G_m C_m + G_{xo} C_{xo} + G_t C_t, \qquad \text{(Eq. 7-6)}$$

$$C_{IM} = G'_m C_m + G'_{xo} C_{xo} + G'_m C_t, \qquad \text{(Eq. 7-7)}$$

$$R_{SFL} = J_m R_m + J_{xo} R_{xo} + J_t R_t, \qquad \text{(Eq. 7-8)}$$

where m refers to the mud column, xo to the flushed zone, and t to the uncontaminated noninvaded formation; C and R are the conductivities and resistivities, respectively, of these zones; and G, G', and J are the geometrical factors of these zones for the ID, IM, and SFL, respectively; all are a function of the same diameter of invasion, d_i. There are three unknowns in these response equations—R_{xo}, R_t, and d_i. (The diameter of invasion and borehole size automatically define all the geometrical factors.)

Solving the equations from the input of the ID, IM, and SFL measurements will yield d_i, R_{xo}, and R_t. Charts Rint-2, -3, -5, -10, -11, and -12 provide a graphical solution for these terms for combinations of induction measurements and mud conditions (mud type and resistivity contrast).

High-Resistivity Formations

In high-resistivity formations, the conductivity signal measured by the induction tool is very small. After calibration there is still an uncertainty of about ± 2 mmho/m on the standard induction measurements (6FF40, ID, IM, 6FF28). This can represent an error of 20% on the signal from a formation of 100 ohm-m (or 10 mmho/m). This error can be significantly reduced by downhole calibration if a suitable impervious, thick formation of exceedingly high resistivity is present.

The calibration accuracy of the Phasor induction tool is much superior. Its uncertainty is less than ± 0.75 mS/m when operated at 20 kHz and about ± 0.40 mS/m when operated at 40 kHz.

Effect of Dipping Beds

Modern computers have allowed the development of increasingly sophisticated models of resistivity logging tool response to actual logging geometries. A recent study was made to analyze the effect of dipping beds on the induction response.

Fig. 7-24 shows the effect of dip on the ID response for 5- and 10-ft resistive and conductive beds, for 0° to 90° dip angles in 10° increments. The resistivity contrast between the bed and shoulders is 20:1 in all cases. The logs were deconvolved and boosted in the same manner as field logs.

The following conclusions were reached as a result of this study: dip makes beds appear thicker than they are; center-bed R_t readings become averaged with R_t readings become averaged with R_s in a generally predictable but not easily quantified manner; thin beds are more affected than thick beds; and resistive beds are affected more than conductive beds.

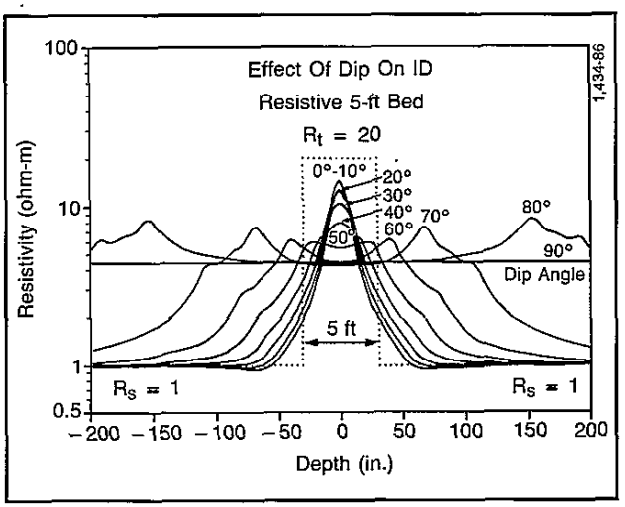

Fig. 7-24a—Effect of dip on ID response in a thin 5-ft resistive bed.

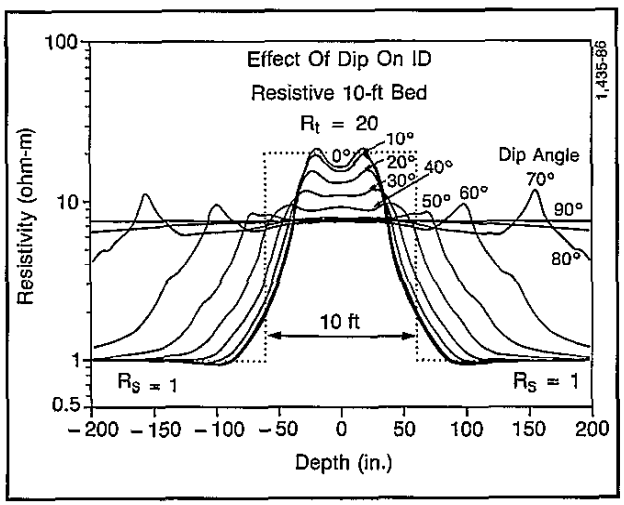

Fig. 7-24b—Effect of dip on ID response in a thick 10-ft resistive bed.

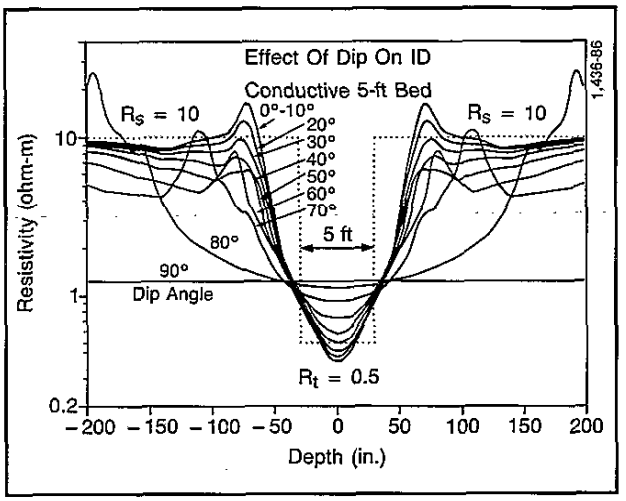

Fig. 7-24c—Effect of dip on ID response in a thin 5-ft conductive bed.

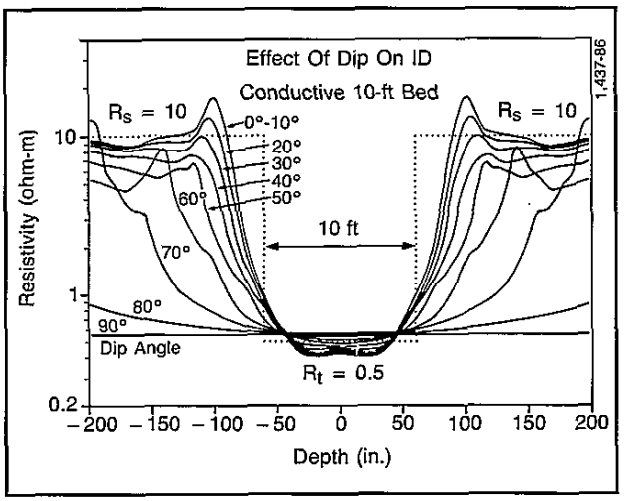

Fig. 7-24d—Effect of dip on ID response in a thick 10-ft conductive bed.

Annulus

In a hydrocarbon-bearing formation of high permeability with very low water saturation, an annulus of high formation water saturation may form between the flushed zone, R_{xo}, and the virgin zone, R_t. If mud filtrate resistivity, R_{mf}, is greater than formation water resistivity, R_w, the annulus may have a resistivity lower than either R_{xo} or R_t; in some cases, its resistivity may be significantly lower. This has the effect of reducing the induction resistivity reading so that an erroneously low value is obtained after applying standard corrections. The effect is most often noted on the IM measurement, but it can influence the ID as well, depending on the exact location of the annulus and its magnitude.

Indeed, there is some evidence that an annulus exists to some degree in most, if not all, hydrocarbon-bearing formations. In most, however, its effect on the induction measurements is negligible. During the drilling of the well, the annulus can wax and wane and move. Thus, in a given formation it may be quite evident on one logging run but essentially absent on another.

Salt Muds

Fig. 7-19 shows that the geometrical factor of all material within a 65-in.-diameter cylinder of the ID array is about 0.2. If R_{xo} is equal to 4 R_t, then C_{xo} equals $C_t/4$, and the induction tool response is

$$\begin{aligned} C_{ID} &= G_{xo}C_{xo} + G_tC_t \\ &= (0.2)\ (C_t/4) + (0.8)\ C_t \\ &= 0.85\ C_t. \end{aligned}$$

In the same conditions, but using salty mud so that R_{xo} equals $R_t/4$, the response is

$$\begin{aligned} C_{ID} &= (0.2)\ 4\ C_t + (0.8)\ C_t \\ &= 1.6\ C_t, \end{aligned}$$

which illustrates the "conductivity-seeking" characteristic of the induction devices and shows why they must be used with discretion in salt-mud environments. As a rule, R_t should be less than about 2.5 R_{xo} and d_i no greater than 100 in. for satisfactory R_t determination from deep induction logs.

However, if formation resistivities are low, invasion is shallow, and the borehole is to gauge and 9 in. or less, the induction tool may perform quite satisfactorily in salt mud.

Phasor Induction SFL Tool

The Phasor Induction SFL tool uses a conventional dual induction-SFL array to record resistivity data at three depths of investigation. In addition to the usual inphase (R-signal) induction measurements, the tool makes a high-quality measurement of the induction quadrature signal (X-signals). These measurements are combined with new advances in signal processing to provide a dual induction SFL log with thin-bed resolution down to 2 ft, and with full correction for such environmental distortions such as shoulder effect and borehole effect.

Since its introduction in the early 1960's, the dual induction tool has evolved into the primary logging service for openhole formation evaluation in fresh and oil-based muds. Previous tools have, however, produced logs with response limitations. These limitations have usually required tedious hand correction. In extreme cases tool response limitations have produced features on logs that were mistaken for geological features. Although the distortions of the formation resistivity caused by resolution effect and shoulder effect are fully predictable from electromagnetic theory, automatic correction algorithms were not successful before now because of the nonlinearity of the R-signal measurement, which was the only measurement made in the older tools.

New developments in electronics technology, recent work on computing the response of the induction tool in realistic formation models, and modern signal processing theory have combined to allow the development of the newer tool which is able to overcome the limitations of previous tools.

Central to this development is a nonlinear deconvolution technique that corrects the induction log in real time for shoulder effect and improves the thin-bed resolution over the full range of formation conductivities. This algorithm, called Phasor Processing, requires the use of the induction quadrature signals, or X-signals, which measure the nonlinearity directly. Phasor Processing corrects for shoulder effect and provides thin-bed resolution down to 2 ft in many cases.

By adding borehole geometry measurements in the same tool string, borehole effect can also be corrected in real time. With these environmental effects removed, a real-time inversion of the data into a three-parameter invasion model can be done at the wellsite.

The Phasor induction design provides several additional advantages over existing tools. These include improvements in the calibration system, sonde error stability, SFL response, and a reduction of signal and cable noise. Each of these improvements contributes toward providing more accurate formation resistivity measurements over a wider range of resistivity and borehole conditions.

Phasor Tool Description and Features

The Phasor Induction SFL tool can be combined with other cable telemetry tools. Measurements returned to the surface include deep (ID) and medium (IM) R-signals, ID and IM X-signals, SFL voltage and current, SFL focus current, spontaneous potential (SP), SP-to-Armor voltage, and array temperature. All measurements except SP are digitized downhole with high-resolution analog-to-digital converters, and all measure channels are recalibrated every 6 in. during logging.

The operating frequency of the induction arrays is selectable at 10 kHz, 20 kHz, or 40 kHz, with a default frequency of 20 kHz. The tool also provides measurements of important analog signals and continuous monitoring of digital signals as an aid to failure detection and analysis. A schematic of the tool is shown in Fig. 7-25. Depths of investigation and vertical resolution of the measurements is listed on the following page:

Median Radial Depths of Investigation		
(above 100 ohm-m homogeneous formation)		ID: 62 in. (158 cm)
		IM: 31 in. (79 cm)
		SFL: 16 in. (41 cm)
(at 0.1 ohm-m homogeneous formation)		ID: 48 in. (122 cm)
		IM: 26 in. (66 cm)
		SFL:16 in. (41 cm)
Vertical Resolution (bed thickness for full R_t determination—no invasion)		IDPH: 8 ft (246 cm)
		IMPH: 6 ft (185 cm)
	*	IDER: 3 ft (92 cm)
		IMER: 3 ft (92 cm)
	†	IDVR: 2 ft (61 cm)
		IMVR: 2 ft (61 cm)
		SFL: 2 ft (61 cm)

*ER-Enhanced Resolution Phasor
†VR-Very Enhanced Resolution Phasor

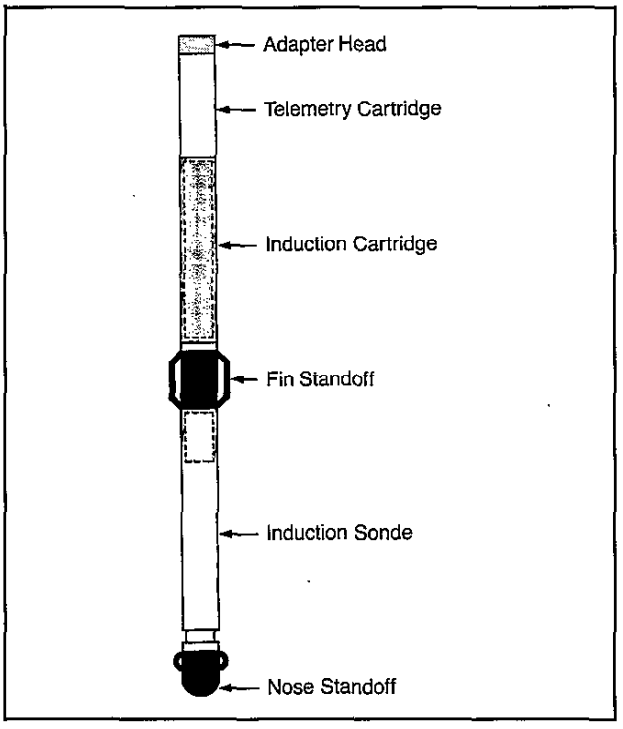

Fig. 7-25—Schematic of the Phasor Induction SFL tool.

Tool design improvements, X-signal measurements, Phasor processing, and borehole corrections provide more accurate resistivity values than other induction tools in all resistivity and bed thickness ranges and borehole conditions. A comparison in the same Texas well between the previous dual induction tool and the Phasor Induction SFL tool with 2-ft vertical resolution (Fig. 7-26) demonstrates the improvement in resolution and accuracy of the Phasor logs.

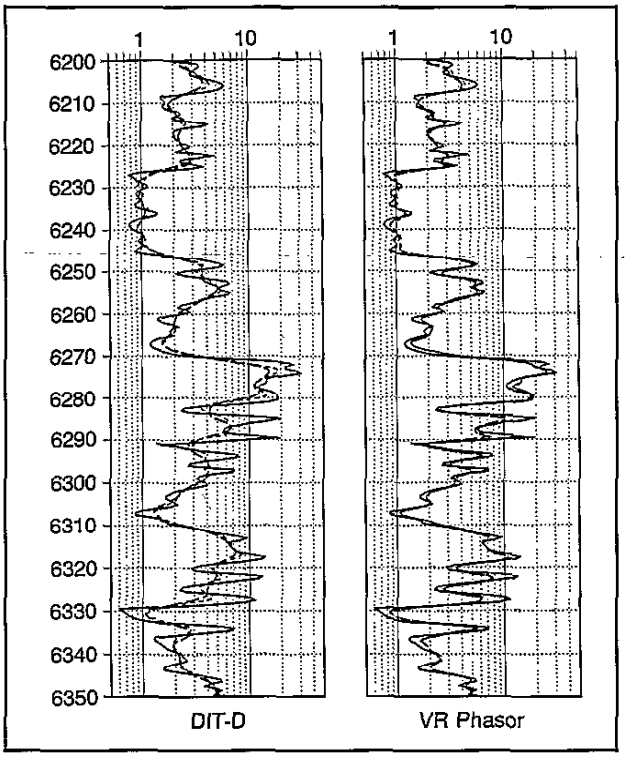

Fig. 7-26—Dual Induction SFL tool recorded in a Texas well versus Phasor Induction SFL tool with 2-ft vertical resolution.

The difference Phasor Processing makes at various resistivity levels is shown in Fig. 7-27a. A set of formation conductivity contrasts produces different response characteristics on the traditional ILD log depending on the average conductivity level. At high resistivity (low conductivity) around 100 ohm-m, the log shows considerable blurring of the thin beds and shoulder effect in the thicker zones. At moderate resistivity, around 10 ohm-m, the log has less shoulder effect. At low resistivity, shoulder effect has disappeared, but the log has developed horns and overshoots. The VR Phasor logs of the same formations (Fig. 7-27b) read correctly regardless of the formation conductivity.

Environmental Corrections

The Phasor Induction tool provides a comprehensive set of automatic corrections for environmental effects. The main ones are:

- Shoulder effect and thin-bed resolution.
- Skin effect.
- Borehole and cave effect.
- Large boreholes.
- Invasion effects.

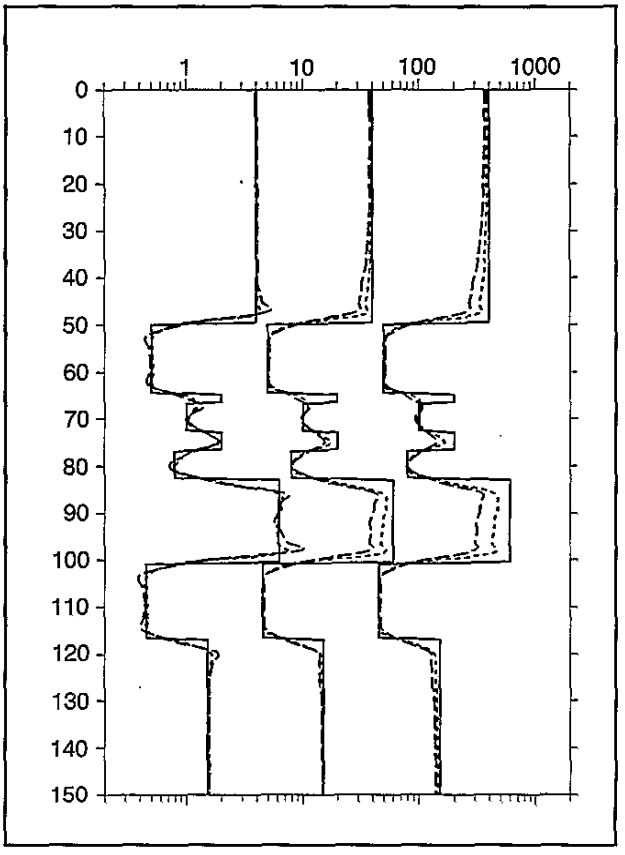

Fig. 7-27a—Varying formation conductivity produces different responses on the traditional ILD measurement.

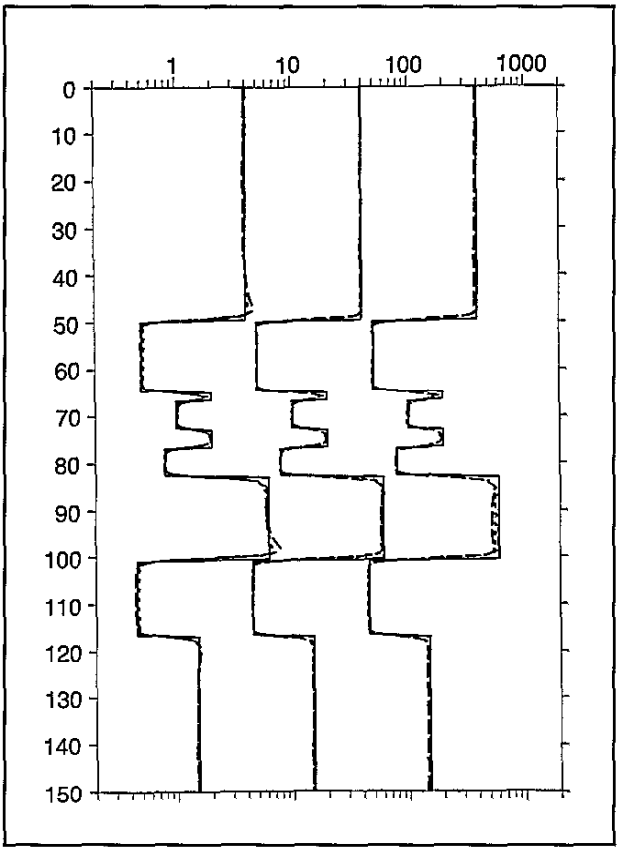

Fig. 7-27b—VR Phasor logs of the same model formations read correctly over the conductivity range.

Shoulder Effect and Vertical Resolution

Shoulder effect is the response of an induction tool to distant conductive beds when in a relatively nonconductive bed thicker than 8 ft. Thin-bed effect appears in beds thinner than the full resolution of ID or IM. The vertical resolution width of the traditional ID is about 8 ft, and IM about 6 ft. The Phasor deconvolution method corrects for shoulder effect and improves thin-bed resolution down to as low as 2 ft.

The ID and IM Phasor logs are available in three vertical resolution "widths": IDPH and IMPH with 8-ft and 6-ft resolution widths to match the resolution of traditional logs, IDER and IMER with 3-ft resolution for improved resolution over a wide range of environmental conditions, and IDVR and IMVR with 2-ft resolution for ultimate resolution over a more limited range of environmental conditions. All Phasor logs are completely corrected for shoulder effect, have vertical response functions that are constant with formation conductivity changes, and have more nearly linear radial responses. Fig. 7-28 shows the improvements of Phasor Processing over traditional processing on the ID measurement for the three resolution widths. These are computed logs in a formation model taken from an Oklahoma well.

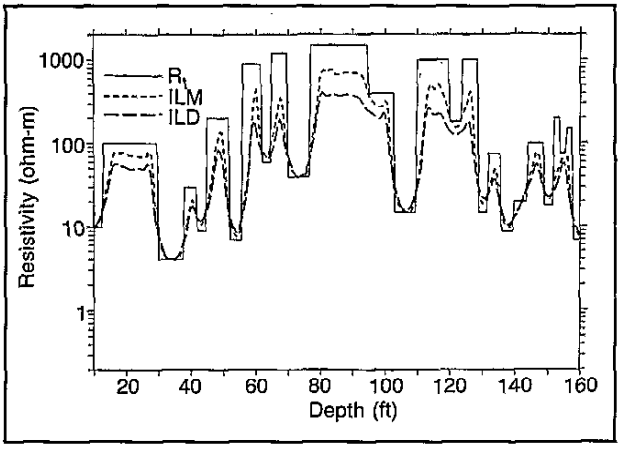

Fig. 7-28a—Traditional dual induction ILD and ILM logs compared to: Phasor IDPH, IMPH.

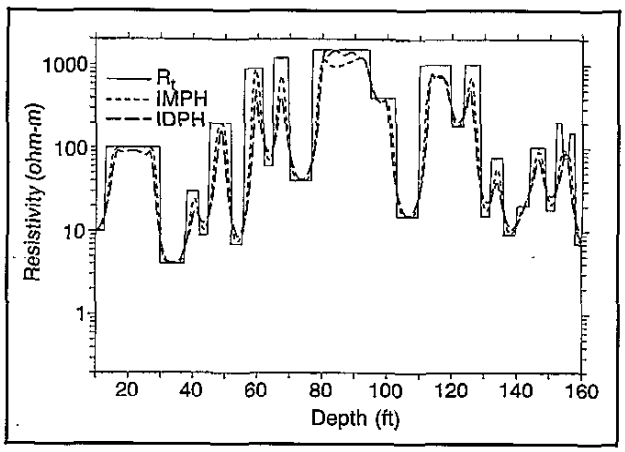

Fig. 7-28b—Traditional dual induction ILD and ILM logs VR Phasor IDER, IMER.

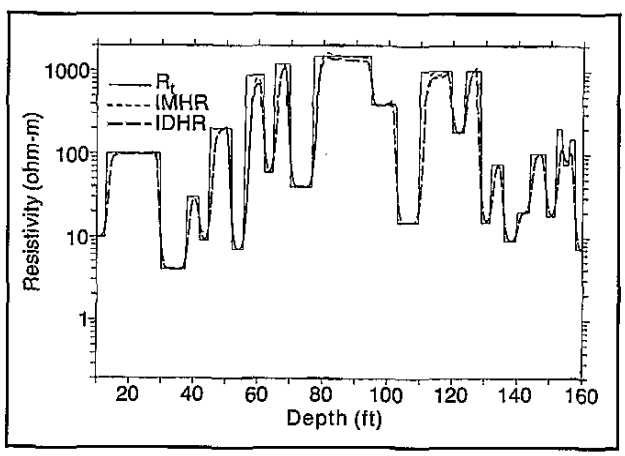

Fig. 7-28c—Traditional dual induction ILD and ILM logs VR Phasor.

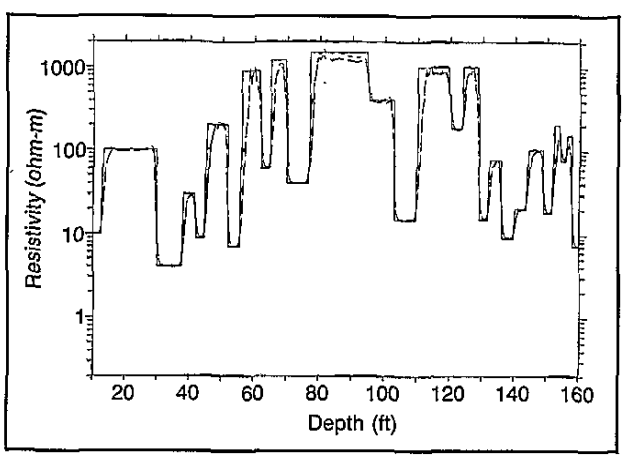

Fig. 7-28d—Traditional dual induction ILD and ILM logs and IDVR, IMVR.

Skin Effect

The problems at low resistivity are more related to skin effect than the problems at high resistivities. The Phasor ID measurement, with skin effect corrected by the X-signal, can read as low as 0.05 ohm-m.

Skin effect is more subtle than the lowest conductivity a tool can read. A log example from a Gulf Coast well is displayed in Fig. 7-29 showing the ID with traditional and VR Phasor Processing. The traditional log shows overshoot at the bed boundaries and incorrect center-bed readings. The VR Phasor log shows that the overshoot problems have been corrected and center-bed improvements made. Note how the IDVR and IMVR curves are parallel.

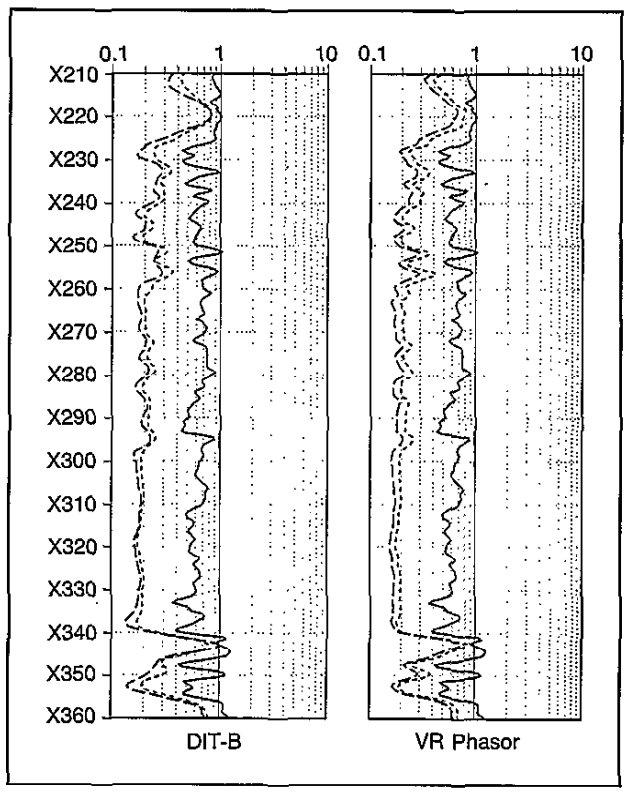

Fig. 7-29—Gulf Coast well with traditional induction ILD, ILM (left), and VR Phasor Processing IDVR, IMVR (right).

Borehole and Cave Effect

Since the induction tool is a "conductivity seeking" device, it can respond strongly to high conductivity in the borehole. Charts for previous tools were based on data determined experimentally and are valid only in smooth holes. Models have been developed that compute the borehole signal with arbitrary formation and borehole conductivities, and in any borehole size and at any standoff. These correction algorithms for the Phasor Induction SFL tool are available for real-time logging. The algorithms use measured information

about the borehole environment, such as hole diameter and borehole conductivity, to determine the correction needed at a given depth.

Large Boreholes

The Phasor Induction SFL tool, in conjunction with specially equipped neutron, density, and sonic devices, can provide excellent logs in large boreholes. The example of Fig. 7-30a shows an overlay of the Phasor ID measurements in a well drilled with a 12.5-in. bit and later reamed with a 23-in. bit. Both logs were automatically corrected for shoulder effect and for borehole and cave effect. Comparisons of the ID curves (Fig. 7-30b) and the invasion-corrected R_t values show that the Phasor Induction SFL tool along with the new modeling techniques allows quality log results in large boreholes. The expense of drilling small holes for logging and then reaming for large casing sizes can now be eliminated.

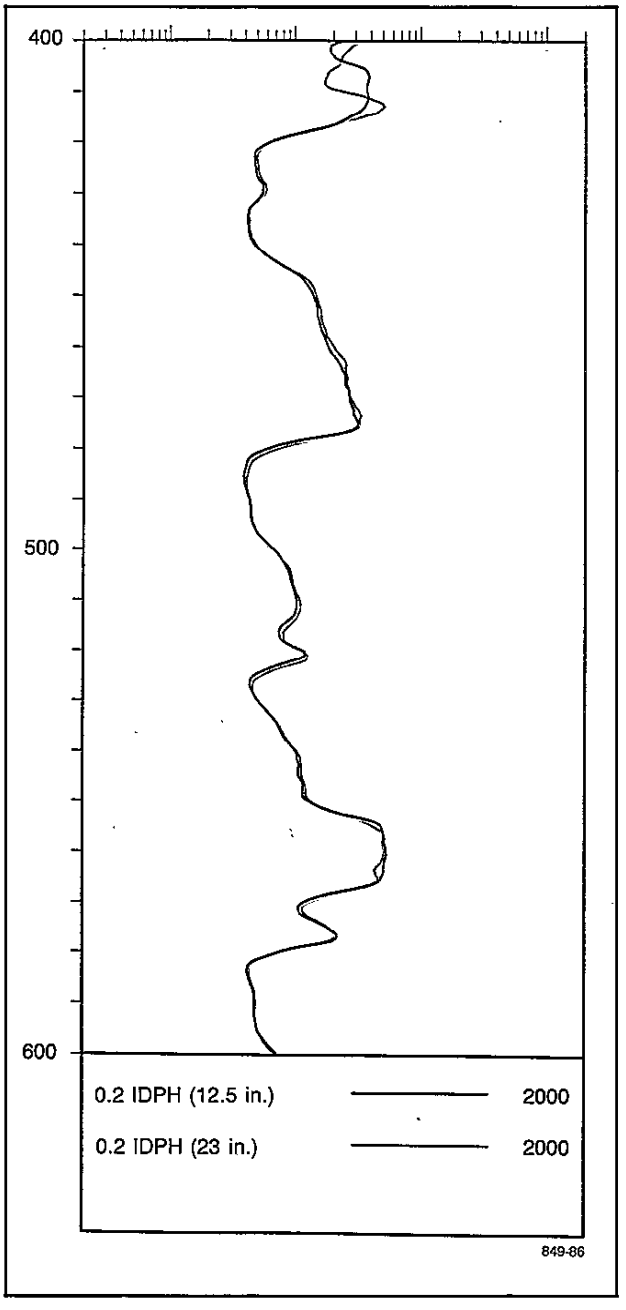

Fig. 7-30a—Phasor IDPH logs in 12.5-in. and 23-in. holes.

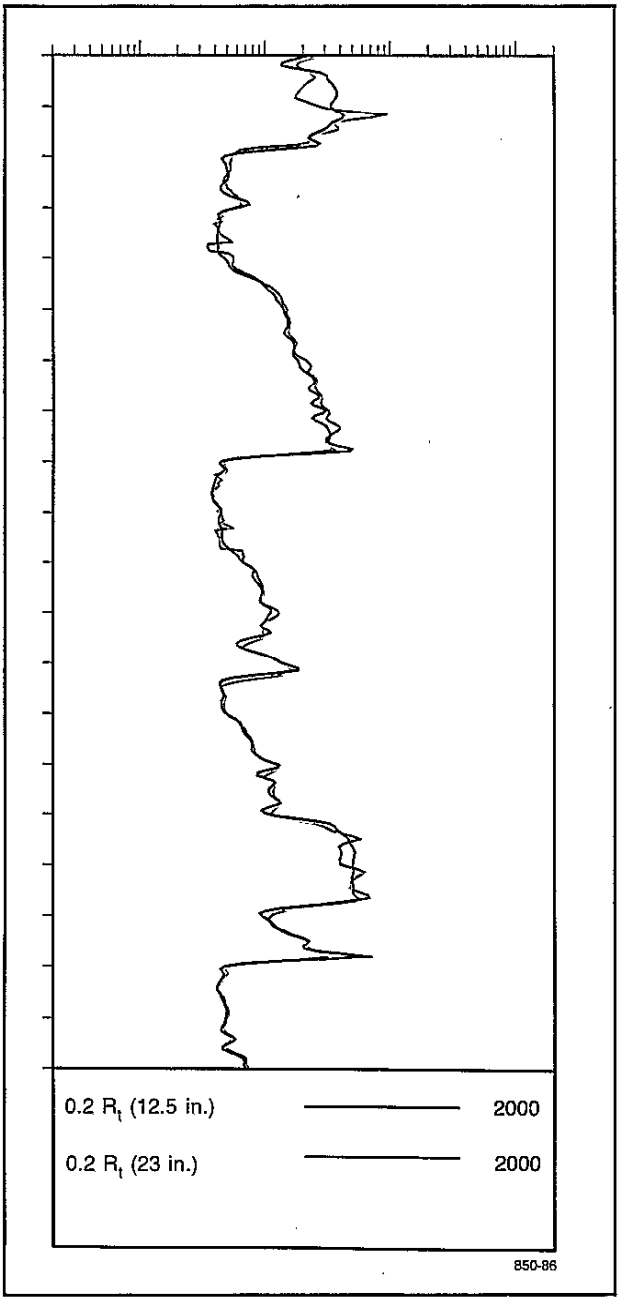

Fig. 7-30b—Invasion-corrected R_t curves.

Invasion Corrections

$R_{xo} > R_t$: the original dual induction tool was developed to determine R_t in the presence of invasion. The three measurements, at three different depths of investigation, are used to solve for parameters of a simple invasion model assuming only a flushed zone and a virgin zone. The solution can be presented in graph form as a "tornado" chart. The Phasor Induction SFL tool has the same task, but, because of the use of the X-signals, the character of the Phasor tornado charts is different. Fig. 7-31 shows the chart for an R_{xo} value of 10 ohm-m. Note that invasion diameters of up to 200 in. can be determined. An algorithm was devised to interpolate between the computed tornado chart data points to produce a log of R_{xo}, R_t, and d_i. Data from cases computed at three R_{xo} values are used in the computation.

$R_{xo} < R_t$: Fig. 7-32 shows a limited set of cases for $R_{xo} < R_t$. Although the recommended tool for these cases has always been the dual laterolog, the figure shows that as long as invasion is moderate, the Phasor induction measurement does a good job. The additional depth of investigation of ID provided by the X-signal aids in separating out these data. The invasion profiling algorithm includes these cases as well as the normal $R_{xo} > R_t$ cases.

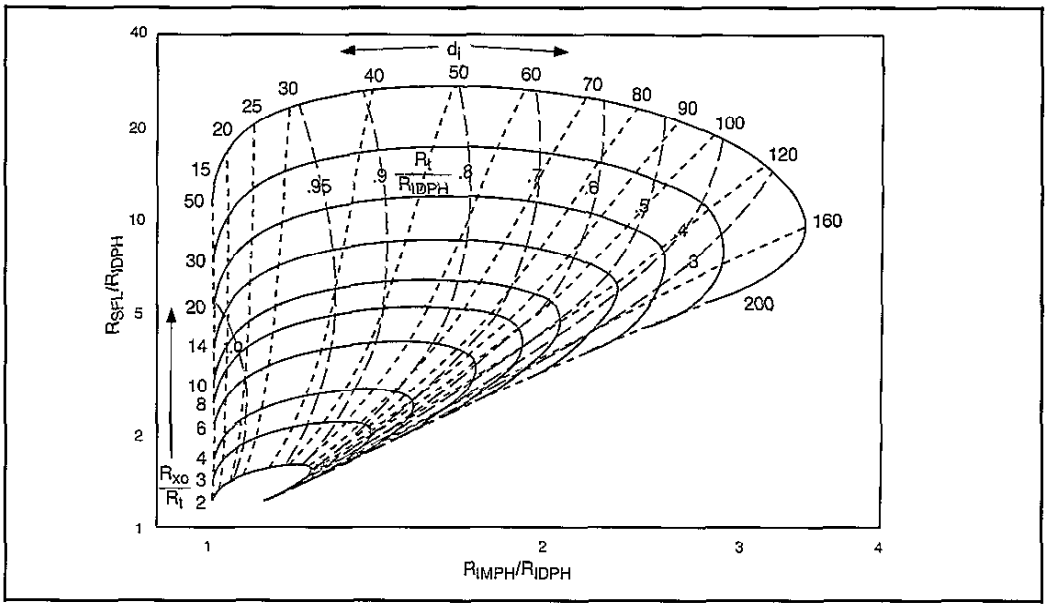

Fig. 7-31—Phasor Induction tornado chart for R_{xo} = 10.

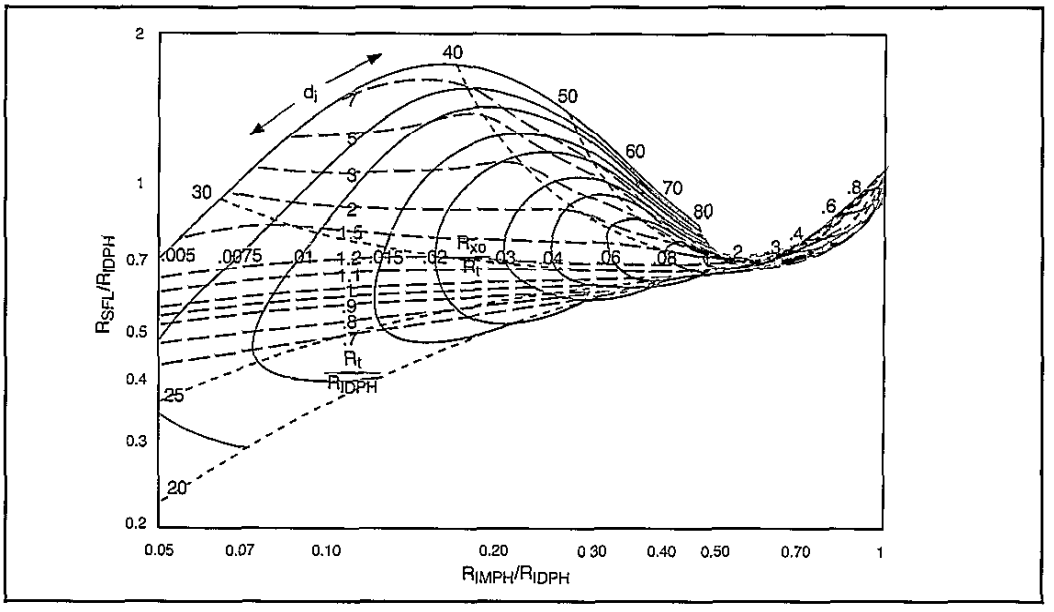

Fig. 7-32—Phasor Induction tornado chart for $R_{xo} < R_t$.

A Phasor log is shown in Fig. 7-33a where the ID measurement in the zone just below 3265 ft reads higher than either the IM or SFL curves. Interpretation through the $R_{xo} < R_t$ chart data produces the R_{xo}, R_t, and d_i log of Fig. 7-33b. A Dual Laterolog-MicroSFL tool was run in this well as the normal resistivity tool for this resistivity regime. The MicroSFL curve, plotted on the invasion-corrected Phasor induction logs, shows the close agreement of the two methods of R_{xo} measurement. For wells where it is expected that some zones will have $R_{xo} < R_t$, the addition of a MicroSFL tool is highly recommended to estimate shallow invasion parameters and to indicate non-step-profile invasion.

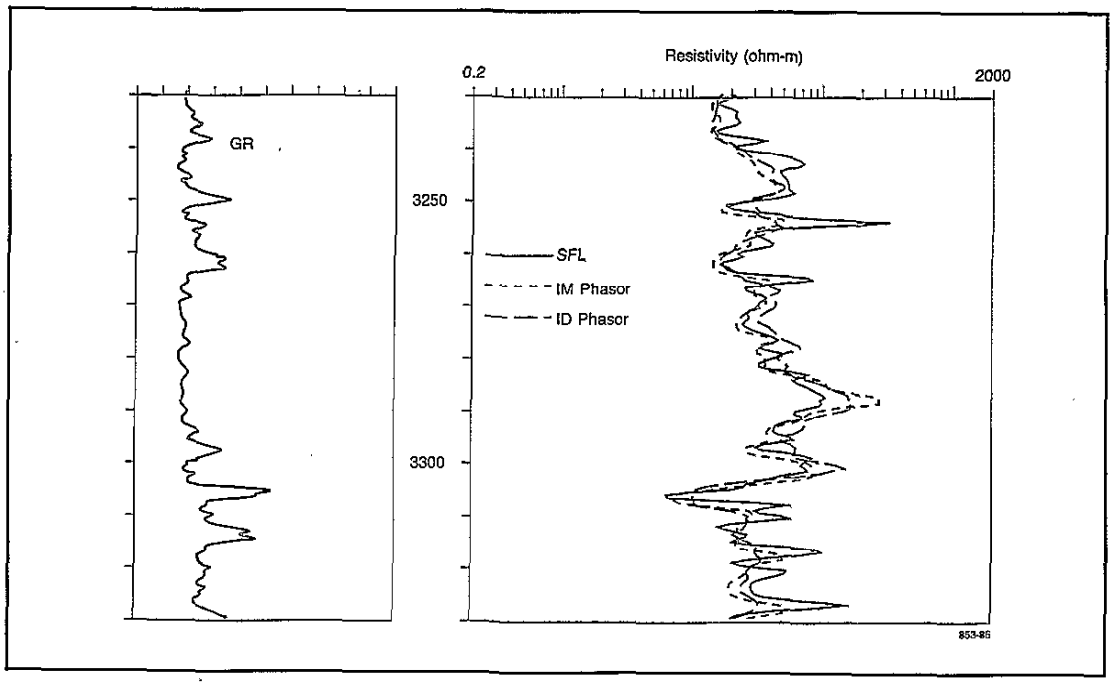

Fig. 7-33a—Phasor log with $R_{xo} < R_t$ zone.

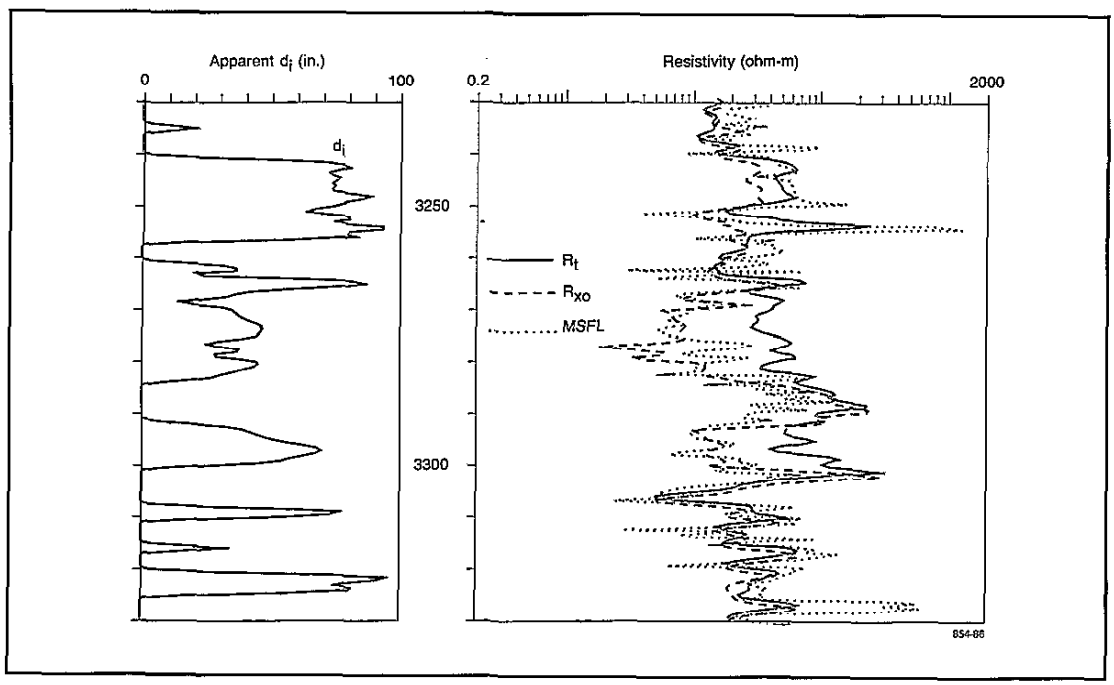

Fig. 7-33b—Phasor invasion interpretation with MicroSFL curve.

Interpretation in the Presence of Transition Zones

Traditional methods of invasion interpretation are based on the assumption of step-profile invasion. The Phasor Induction SFL tool brings new methods of interpretation to more realistic invasion profiles where transition zones can complicate the induction log. Two types of transitions are expected to be common: a "slope" profile with a continuous transition from R_{xo} to R_t over some radial distance, and the annulus profile. Studies[30] have shown that slope profiles produce little error in the estimate of R_t made by tornado chart methods. Annulus profiles can cause significant errors in estimating R_t, but they can be detected by comparison of Phasor logs made at all three operating frequencies, or by the addition of an R_{xo} device such as the MicroSFL tool.[30]

Oil-Based Mud

The Phasor induction service also provides better resistivity values in wells drilled with oil-based mud systems. Establishing an invasion profile requires three measurements with varying depths of investigation. When oil-based mud is used, the SFL device cannot be used for the shallow resistivity measurement, but the Phasor's X-signals provide some additional depth information. Various combinations of the R- and X-signal measurements were tested for invasion interpretation, particularly at shallow invasion diameters. The chart of Fig. 7-34 was the best compromise and is applicable only below 10 ohm-m. Above that resistivity, the X-signals are not sufficiently localized to provide accurate invasion interpretation. Note that the raw, unboosted ID and IM measurements are used as "medium" and "shallow," respectively. The axes are reversed from those of the usual tornado chart.

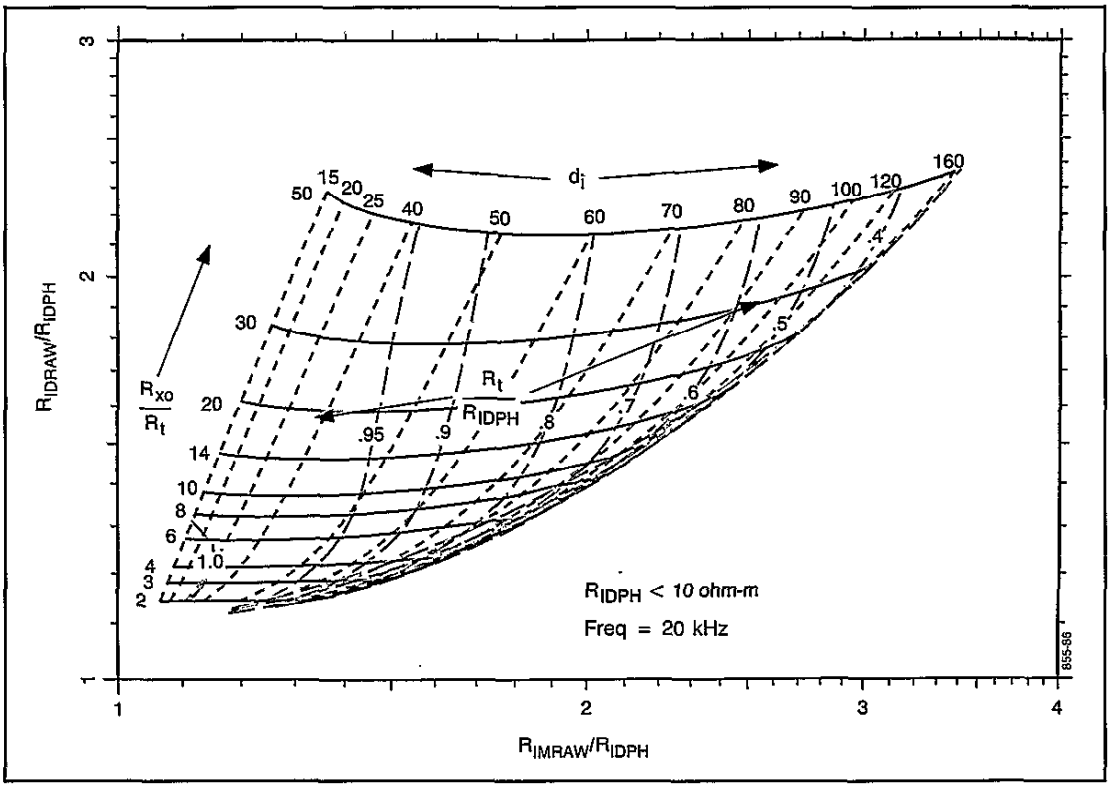

Fig. 7-34—Phasor Induction oil-based mud invasion interpretation, applicable only below 10 ohm-m.

Phasor Case Studies

Case studies illustrate the effectiveness of the Phasor induction measurements and the environmental corrections algorithms.

The first example is from a gas well in Oklahoma, and shows the large errors that can be caused by shoulder effect. The traditional dual induction log is shown in Fig. 7-35a. The zones from 9255 to 9295 ft and 9490 to 9540 ft are low-porosity limestone with gas production from fractures; the log exhibits classic shoulder effect on ID and IM, with both tools seeing the very conductive shoulders. The environmentally corrected Phasor (7-ft) logs are shown in Fig. 7-35b. Borehole effect in these zones is negligible, so all the differences come from the Phasor shoulder-effect correction. The invasion correction is shown in Fig. 7-35c, with R_t, R_{xo}, and an apparent d_i resulting from the tornado chart algorithm.

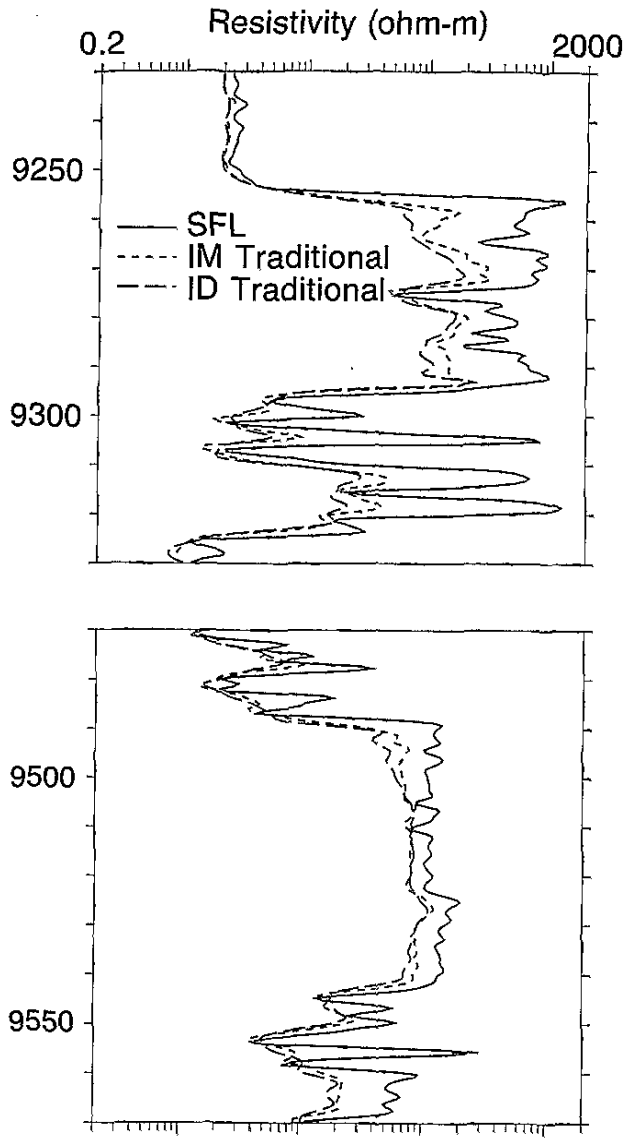

Fig. 35a—Dual Induction SFL log.

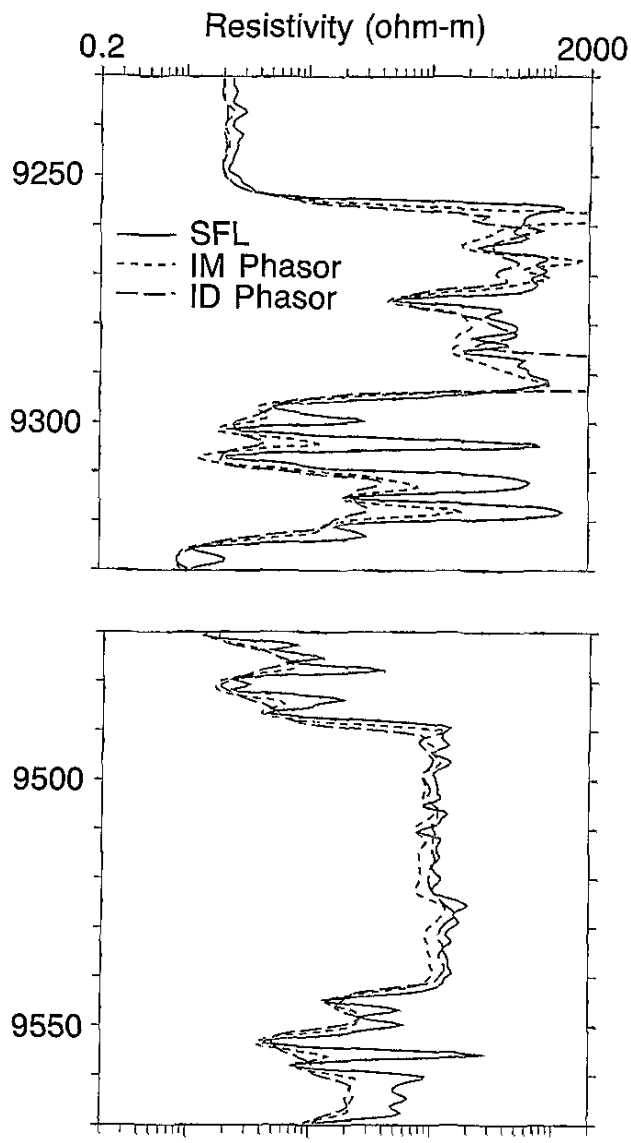

Fig. 35b—Phasor Processed (7-ft) log.

The corrections shown are what one expects from the published thin-bed charts; however, the best test of the corrections is a computed log with a known input formation. Fig. 7-35d shows a computed ID log designed to resemble the zone in the previous example. The solid rectangular curve shows the input formation. The short dashed curve shows the ID as traditionally processed, while the long dashed curve shows the ID Phasor Processed. The Phasor ID curve shows no shoulder effect and agrees with the input formation to better than 0.5 mS/m.

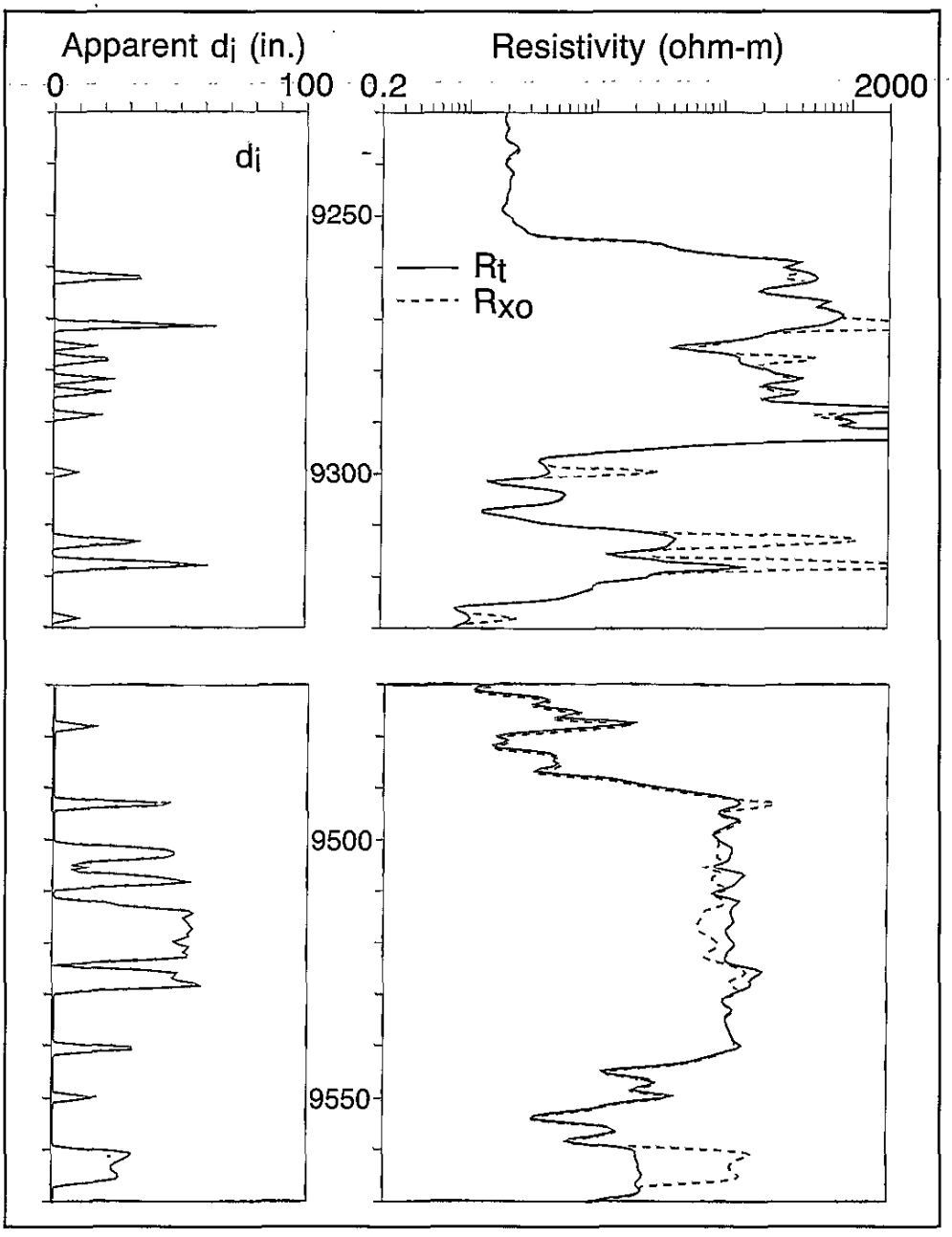

Fig. 7-35c—Phasor invasion interpretation.

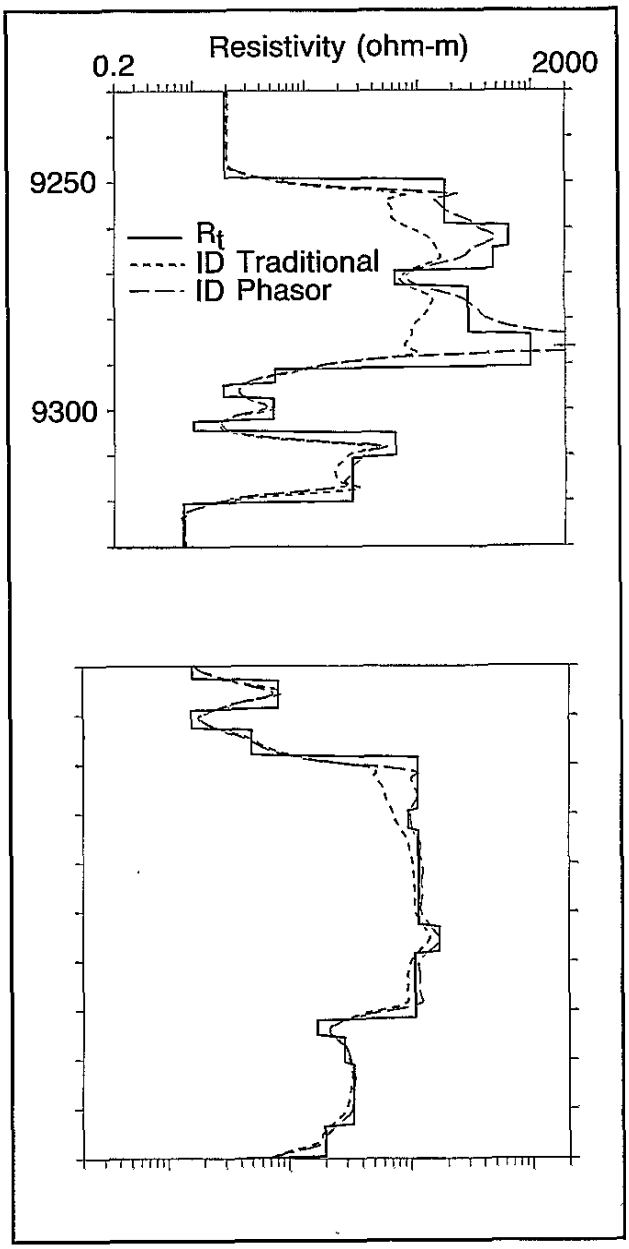

Fig. 7-35d—Computed log showing effect of Phasor Processing.

Another comparison is shown by an Offshore Gulf of Mexico well; Fig. 7-36 shows the traditional dual induction log from this well. Note the zone near 10560 ft with the SFL measurement showing a series of thin beds and the ILD curve anticorrelating with the SFL curve. The VR Phasor (2-ft) log clearly delineates the beds. The invasion interpretation of Fig. 7-36b shows the invaded laminations.

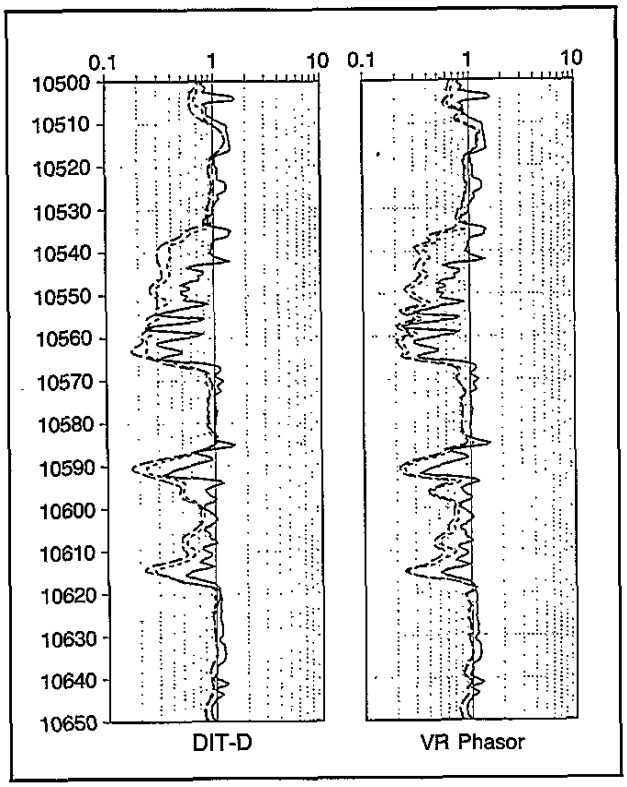

Fig. 7-36a—Offshore Gulf of Mexico well with traditional DIL and VR Phasor (2-ft) log which clearly delineates thin beds.

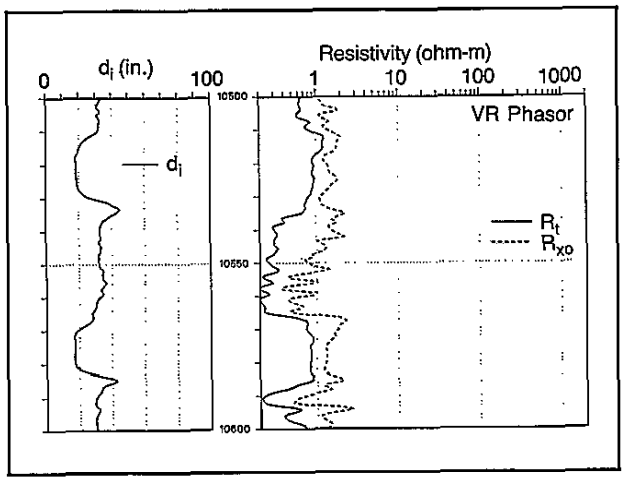

Fig. 7-36b—Phasor invasion interpretation of zone at 10,550 ft.

The third example is from a Canadian well with high resistivities from 125 to 130 m in a dolomitic sandstone which produces water-free gas. Figure 37a shows the traditional logs,

Fig. 37b shows the nuclear logs, and Fig. 37c shows the ER Phasor (3-ft) logs over the interval. ER Phasor logs predict an S_w of 12-14%, a significant reduction from the S_w of about 20% from the traditional logs. The ER Phasor logs also delineate the individual beds within the reservoir.

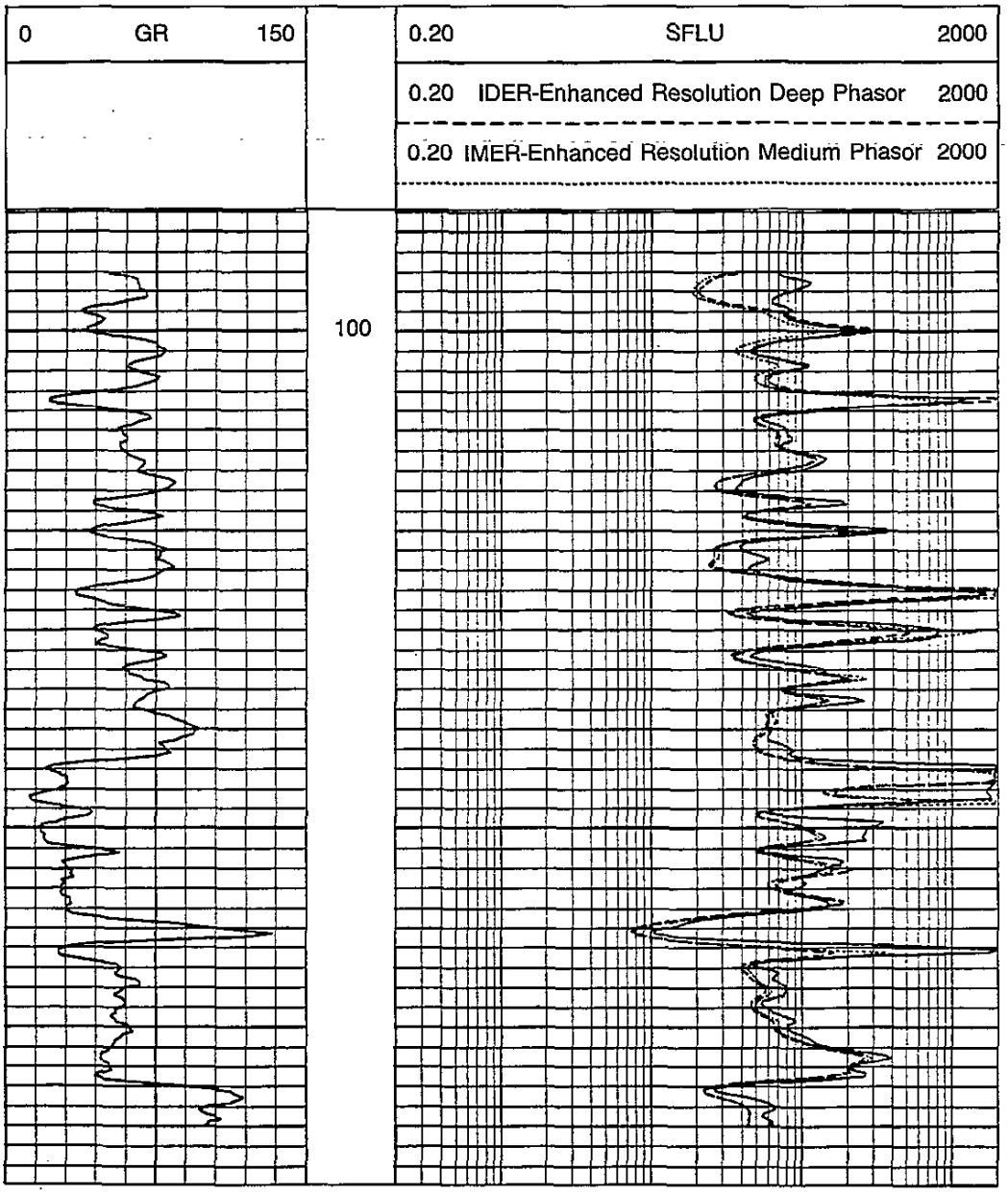

Fig. 7-37a—Canadian well with high resistivities recorded by traditional DIL.

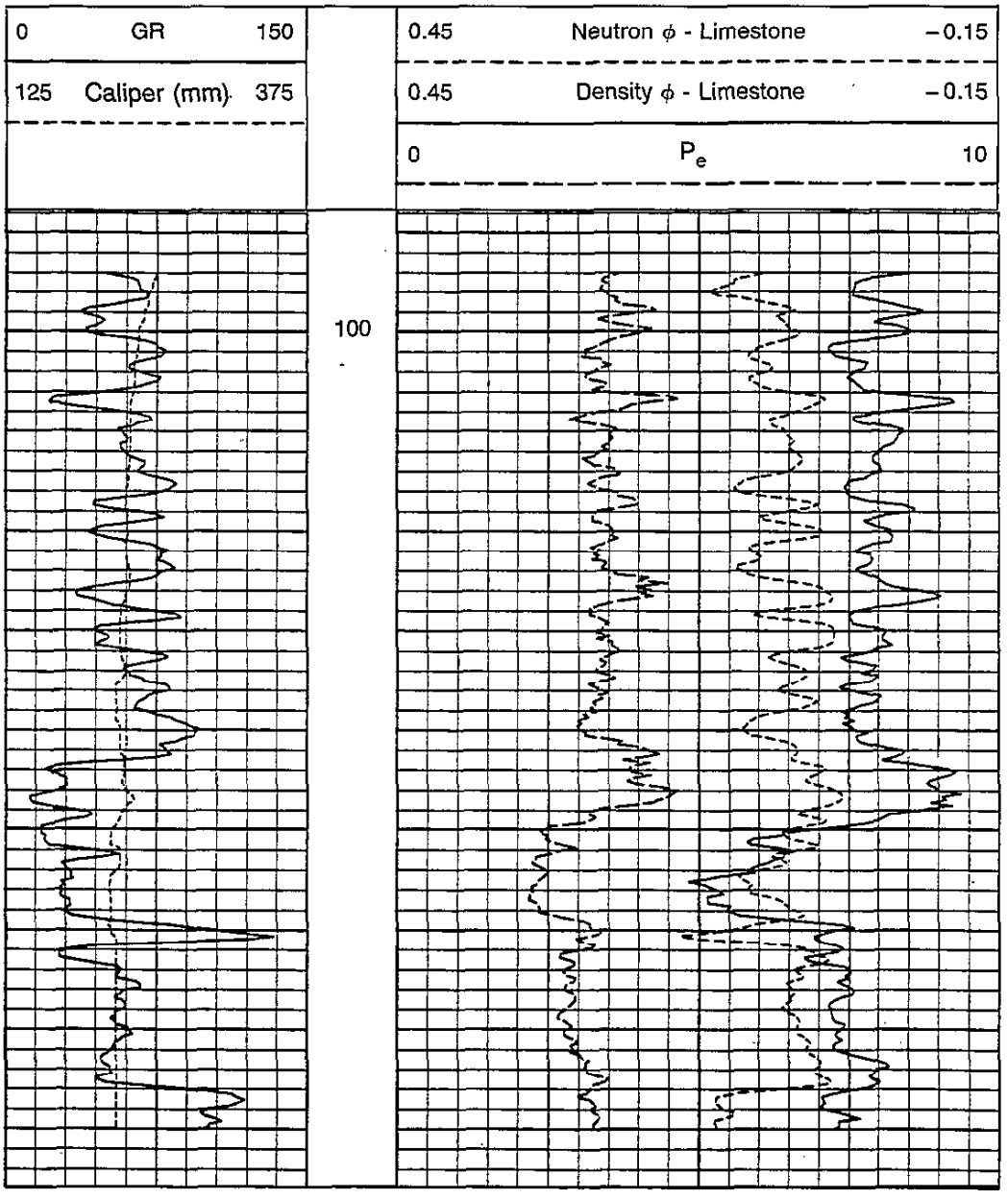

Fig. 7-37b—Nuclear logs reveal dolomitic sandstone which produces water-free gas.

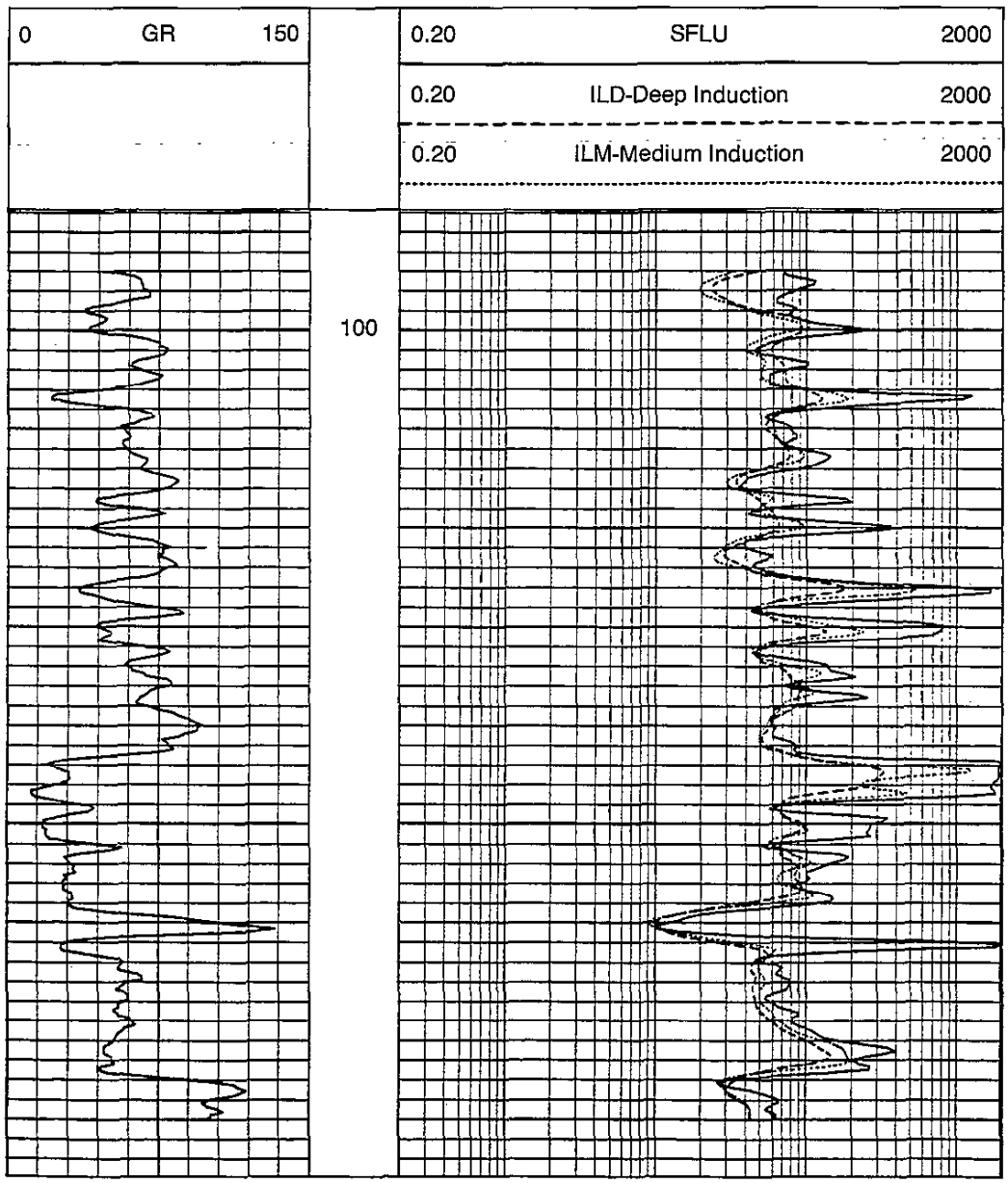

Fig. 7-37c—ER Phasor (3-ft) log with improved resistivity and bed definition.

Induction Versus Laterolog Measurements

Nearly all resistivity measurements are now made with focused devices. These tools are designed to minimize the influence of the borehole fluid and surrounding beds. Two types of tools exist: laterolog and induction tools. They have unique characteristics that favor their use in specific, and often different, situations and applications.

The induction log is generally recommended in holes drilled with only moderately conductive drilling muds, nonconductive muds (e.g., oil-base muds), and in empty or air-drilled holes. The laterolog is generally recommended in holes drilled with very conductive drilling muds (i.e., salt muds).

The induction tool, being a conductivity-sensitive device, is most accurate in low- to medium-resistivity formations. The laterolog tool, being a resistivity device, is most accurate in medium- to high-resistivity formations.

There is an overlap in the areas of applicability. The chart of Fig. 7-38 has been constructed for average cases: d_i from 0 to 80 in. and the possible occurrence of an annulus. This chart is only a guide. For conditions other than those given, the areas of applicability may differ.

As seen from Fig. 7-38, the laterolog measurement is preferred when R_{mf}/R_w falls to the left of the vertical dashed line and to the left of the solid line for the appropriate value of R_w. The induction log is preferred above the appropriate R_w line. To the right of the dashed line and below the appropriate R_w curve, either or both logs may be required for an accurate interpretation.

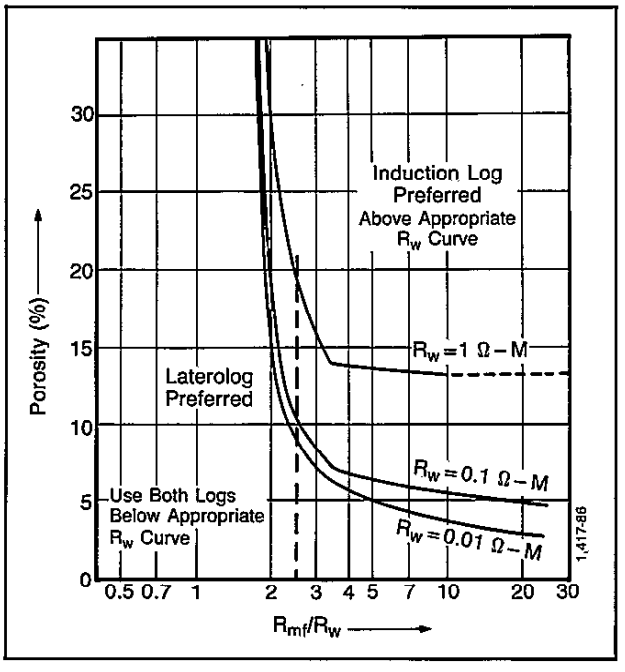

Fig. 7-38—Preferred ranges of application of induction logs and laterologs for usual cases.

The nature of the two tools can be described simply by saying that laterolog devices "see" the more resistive zones; induction tools "see" the more conductive zones. Thus R_{xo} is greater than R_t, the induction tool is preferred for R_t determination, and the laterolog tool is preferred where R_{xo} is less than R_t. Since the induction tool is a conductivity-seeking device it responds strongly to high conductivity in the borehole. Recent modeling efforts have led to codes that compute the borehole signal with arbitrary formation and borehole conductivities, and in any borehole size and at any standoff. A caliper, recorded with the induction tool, is required for the borehole correction.

The results of this method are shown in Fig. 7-39. The well drilled with salty mud was logged with the Phasor induction tool and the DLL tool. The ID log was first corrected for shoulder effect with the Phasor algorithm, then corrected for borehole effect. The resistivity spike at 3057 ft on the uncorrected ID measurement is due to borehole signal; the spikes at 3112 and 3123 are a result of cave effect. The ID log uncorrected is not very useful. After correction, it is much closer to the LLD curve. Although the laterolog tool is preferred in these conditions, the induction log provides acceptable results in this extreme case with Phasor Processing.

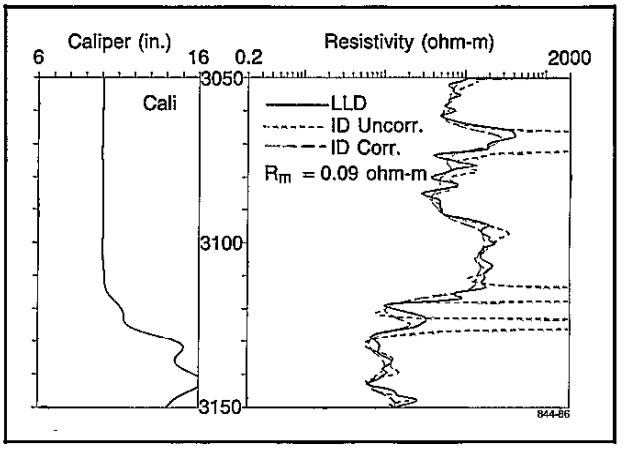

Fig. 7-39—Field log with and without borehole correction.

Induction logs provide acceptable thin-bed resolution, which makes reliable formation evaluation possible in beds down to 3-ft thick (IDER, IMER). The laterolog devices exhibit even better thin-bed resolution. Except for beds with extremely high resistivity, reliable formation evaluation is possible in beds as thin as 3 ft.

Both laterolog and induction measurements are influenced by the borehole and by surrounding beds. Even relatively thick beds may have some effect on their measurements. The measurements of both devices should be corrected for

borehole and surrounding bed effects. Although these corrections are usually small, it is good practice to make them to insure that they are not overlooked in those few cases where they are significant.

To correct either the LLD or the ID measurements for invasion effects, at least three resistivity measurements of differing depths of investigation are required. It is, therefore, strongly recommended that the resistivity log include at least three resistivity measurements. For the laterolog system, this could consist of a DLL-R_{xo} log (LLD, LLS, and MicroSFL measurements). For the induction system, this could consist of the DIL-SFL (ID, IM, and SFL) or, better yet, the Phasor Induction SFL tool (IDPH, IMPH, and SFL).

MICRORESISTIVITY DEVICES

Microresistivity devices are used to measure the resistivity of the flushed zone, R_{xo}, and to delineate permeable beds by detecting the presence of mudcake.

Measurements of R_{xo} are important for several reasons. When invasion is moderate to deep, a knowledge of R_{xo} allows the deep resistivity measurement to be corrected to true formation resistivity. Also, some methods for computing saturation require the R_{xo}/R_t ratio. In clean formations, a value of F can be computed from R_{xo} and R_{mf} if S_{xo} is known or can be estimated.

To measure R_{xo}, the tool must have a very shallow depth of investigation because the flushed zone may extend only a few inches beyond the borehole wall. Since the reading should not be affected by the borehole, a sidewall-pad tool is used. The pad, carrying short-spaced electrode devices, is pressed against the formation and reduces the short-circuiting effect of the mud. Currents from the electrodes on the pad must pass through the mudcake to reach the flushed zone.

Microresistivity readings are affected by mudcake; the effect depends on mudcake resistivity, R_{mc}, and thickness, h_{mc}. Moreover, mudcakes can be anisotropic, with mudcake resistivity parallel to the borehole wall less than that across the mudcake. Mudcake anisotropy increases the mudcake effect on microresistivity readings so that the effective, or electrical, mudcake thickness is greater than that indicated by the caliper.

Older microresistivity equipment included a tool with two pads mounted on opposite sides. One was the microlog pad, and the other was either the microlaterolog or Proximity pad, as required by mud and mudcake conditions. The measurements were recorded simultaneously.

Newer microresistivity equipment includes a microlog tool and a MicroSFL tool. Mounted on the powered caliper device, the microlog can be run simultaneously with any combination of Litho-Density*, CNL*, DIL, NGS, or EPT* logging services.

* *Mark of Schlumberger*

The MicroSFL tool can also be run in combination with other services. It is most commonly combined with the DLL or DIL equipment.

Microresistivity logs are scaled in resistivity units.

- When recorded by itself, the microlog is usually recorded over Tracks 2 and 3 on a linear scale. The microcaliper is shown in Track 1.
- The microlaterolog and Proximity logs are recorded on a four-decade logarithmic scale to the right of the depth track (Fig. 7-40). The caliper is recorded in Track 1. When the microlog is also recorded, it is presented in Track 1 on a linear scale.
- The MicroSFL measurement is also recorded on the logarithmic grid. When run with the DLL or DIL log, it is presented on the same film and on the same resistivity scale.

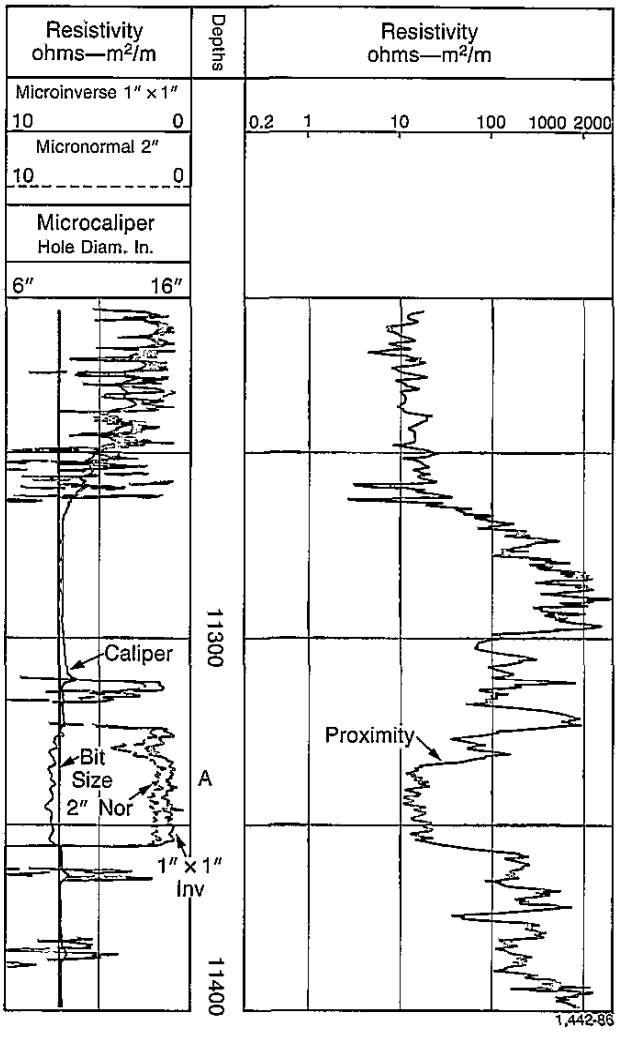

Fig. 7-40—Presentation of Proximity-Microlog.

Microlog

With the microlog tool, two short-spaced devices with different depths of investigation provide resistivity measurements of a very small volume of mudcake and formation immediately adjoining the borehole. Comparison of the two curves readily identifies mudcake, which indicates invaded and, therefore, permeable formations.

Principle

The rubber microlog pad is pressed against the borehole wall by arms and springs. The face of the pad has three small in-line electrodes spaced 1 in. apart. With these electrodes a 1- by 1-in. microinverse ($R_{1"x1"}$) and a 2-in. micronormal ($R_{2"}$) measurement are recorded simultaneously.

As drilling fluid filters into the permeable formations, mud solids accumulate on the hole wall and form a mudcake. Usually, the resistivity of the mudcake is slightly greater than the resistivity of the mud and considerably lower than the resistivity of the invaded zone near the borehole.

The 2-in. micronormal device has a greater depth of investigation than the microinverse. It is, therefore, less influenced by the mudcake and reads a higher resistivity, which produces "positive" curve separation. In the presence of low-resistivity mudcake, both devices measure moderate resistivities, usually ranging from 2 to 10 times R_m.

In impervious formations, the two curves read similarly or exhibit some "negative" separation, and the resistivities are usually much greater than in permeable formations.

Interpretation

Positive separation in a permeable zone is illustrated in Fig. 7-40 at Level A. The caliper shows evidence of mudcake. Although the microlog curves identify permeable formations, quantitative inferences of permeability are not possible.

When no mudcake exists, the microlog readings may yield useful information about borehole condition or lithology, but the log is not quantitatively interpretable.

Under favorable circumstances, R_{xo} values can be derived from the microlog measurements using Chart Rxo-1. R_{mc} values for this purpose can be measured directly or estimated from Chart Gen-7, and h_{mc} is obtained from the caliper curve. Limitations of the method are:

- The ratio R_{xo}/R_{mc} must be less than about 15 (porosity more than 15%).
- h_{mc} must be no greater than 0.5 in.
- Depth of invasion must be over 4 in.; otherwise, the microlog readings are affected by R_t.

Microlaterolog

The microlaterolog tool was designed to determine R_{xo} accurately for higher values of R_{xo}/R_{mc} where the microlog interpretation lacks resolution.

Principle

The microlaterolog pad is shown in Fig. 7-41. A small electrode, A_O, and three concentric circular electrodes are embedded in a rubber pad applied against the hole wall. A constant current, i_o, is emitted through A_O. Through the outer electrode ring, A_1, a varying current is emitted and automatically adjusted so that the potential difference between the two monitoring electrode rings, M_1 and M_2, is maintained essentially equal to zero. The i_o current is forced to flow in a beam into the formation. The resulting current lines are shown on the figure. The i_o current near the pad forms a narrow beam, which opens up rapidly a few inches from the face of the pad. The microlaterolog resistivity reading is influenced mainly by the formation within this narrow beam.

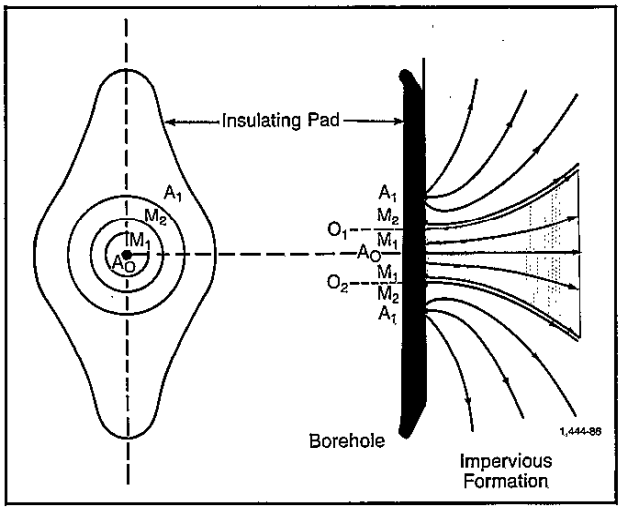

Fig. 7-41—Microlaterolog pad showing electrodes (left) and schematic current lines (right).

Fig. 7-42 compares qualitatively the current-line distributions of the microlaterolog and the microlog devices when the corresponding pad is applied against a permeable formation. The greater the value of R_{xo}/R_{mc}, the greater the tendency for the microlog i_o current to escape through the mudcake to the mud in the borehole. Consequently, for high R_{xo}/R_{mc} values, microlog readings respond very little to variations of R_{xo}. On the contrary, all the microlaterolog i_o current flows into the permeable formation and the microlaterolog reading depends mostly on the value of R_{xo}.

Response

Laboratory tests and computer simulation results have shown that the virgin formation has practically no influence on the microlaterolog readings if the invasion depth is more than 3 or 4 in.

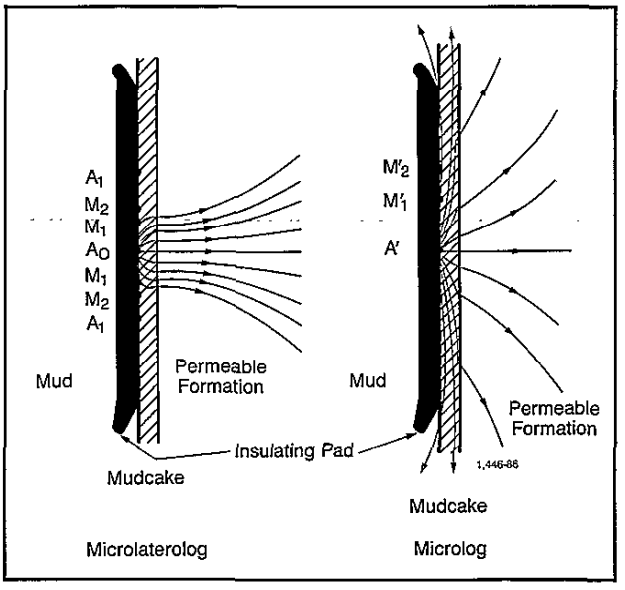

Fig. 7-42—Comparative distribution of current lines of Microlaterolog and Microlog.

The influence of mudcake is negligible for mudcakes less than ⅜ in., but increases rapidly with greater thicknesses. Chart Rxo-2 (top) gives appropriate corrections.

Proximity Log

Principle

The Proximity tool is similar in principle to the microlaterolog device. The electrodes are mounted on a wider pad, which is applied to the wall of the borehole; the system is automatically focused by monitoring electrodes.

Response

Pad and electrode design are such that isotropic mudcakes up to ¾ in. have very little effect on the measurements (see Chart Rxo-2, bottom).

The Proximity tool has a significantly deeper depth of investigation than does the microlog or microlaterolog tools. Thus, if the invasion is very shallow, the Proximity measurement may be influenced by R_t. The resistivity measured can be expressed as:

$$R_P = J_{xo} R_{xo} + (1 - J_{xo}) R_t ,$$

where R_P is resistivity measured by the Proximity log and J_{xo} is the pseudogeometrical factor of the flushed zone. The value of J_{xo}, as a function of invasion diameter, d_i, is given in Fig. 7-43; this chart gives only an approximate value of J_{xo}. J_{xo} depends, to some extent, on the diameter of the borehole and on the ratio R_{xo}/R_t.

If d_i is greater than 40 in., J_{xo} is very close to unity; accordingly, the Proximity log measures R_{xo} directly. If d_i is less than 40 in., R_P is between R_{xo} and R_t, usually much closer to R_{xo} than to R_t. R_P can be fairly close to R_t only if the invasion is nonexistent or extremely shallow; of course, when R_{xo} and R_t are similar, the value of R_P depends very little on d_i.

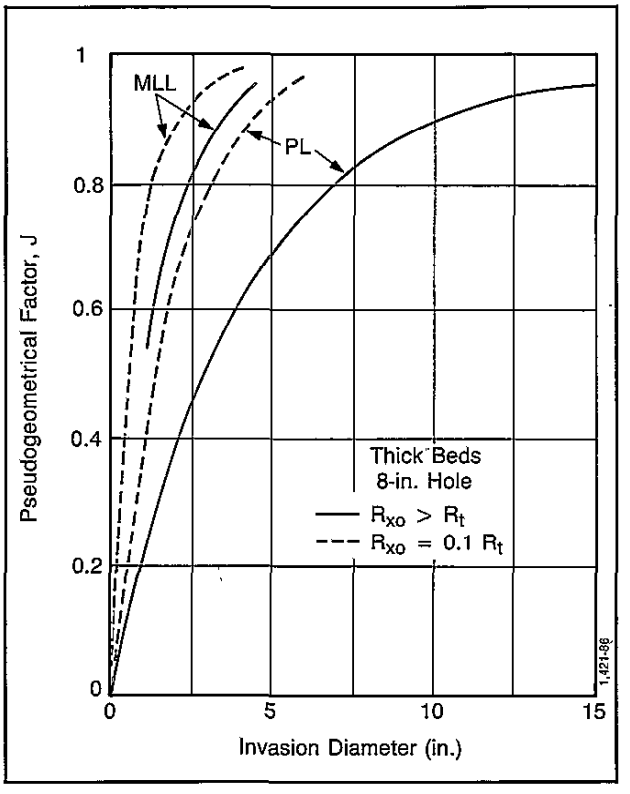

Fig. 7-43—Pseudogeometrical factors, Microlaterolog and Proximity log.

Vertical Resolution

The resolution of the Proximity log is about 6 in. Corrections for the effect of adjacent beds are unnecessary for bed thicknesses greater than 1 ft.

MicroSFL

The MicroSFL is a pad-mounted spherically focused logging device that has replaced the microlaterolog and Proximity tools. It has two distinct advantages over the other R_{xo} devices. The first is its combinability with other logging tools, including the DIL and DLL tools. This eliminates the need for a separate logging run to obtain R_{xo} information.

The second improvement is in the tool's response to shallow R_{xo} zones in the presence of mudcake. The chief limitation of the microlaterolog measurement is its sensitivity

to mudcakes. When mudcake thickness exceeds about ⅜ in., the log readings are severely influenced at high R_{xo}/R_{mc} contrasts. The Proximity log, on the other hand, is relatively insensitive to mudcakes, but it requires an invaded zone with a d_i of about 40 in. in order to provide direct approximations of R_{xo}.

The solution was found in an adaptation of the principle of spherical focusing in a sidewall-pad device. By careful selection of electrode spacings and bucking-current controls, the MicroSFL measurement was designed for minimum mudcake effect without an undue increase in the depth of investigation (see Chart Rxo-3). Fig. 7-44 illustrates, schematically, the electrode arrangement (right) and the current patterns (left) of the MicroSFL tool.

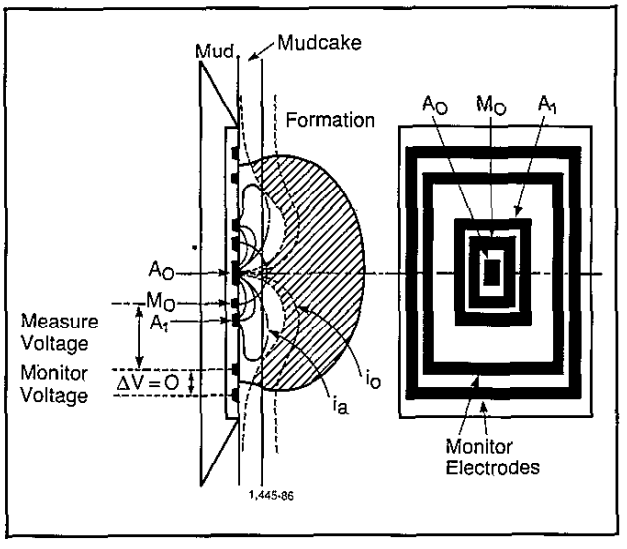

Fig. 7-44—Electrode arrangement of MicroSFL device (right) and current distribution (left).

The surveying current flows outward from a central electrode, A_O. Bucking currents, passing between the electrodes, A_O and A_1, flow in the mudcake and, to some extent, in the formation. The measuring current, i_o, is thereby confined to a path directly into the formation, where it quickly "bells" out and returns to a remote electrode, B. To achieve this, the bucking current is adjusted to make the monitor voltage equal to zero. By forcing the measure current to flow directly into the formation, the effect of mudcake resistivity on tool response is minimized; yet, the tool still has a very shallow depth of investigation.

Synthetic microlog curves can be computed from MicroSFL parameters. Since the measure current sees mostly the flushed zone and the bucking current sees primarily the mudcake, it is possible to mathematically derive micronormal and microinverse curves.

Environmental Corrections

Microresistivity measurements must be corrected for mudcake. Charts Rxo-1, -2, and -3 provide the mudcake correction for the microlog, microlaterolog, Proximity, and MicroSFL values, respectively. The correction is a function of the mudcake thickness and the resistivity contrast between the mudcake and the microresistivity measurement. Mudcake thickness is normally deduced from a comparison of the actual borehole size, as measured with the caliper, to the known bit size.

Resistivity Interpretation

When invasion is very deep an accurate value of R_t is sometimes difficult to measure because the reading of the deep-investigation log is also affected by R_{xo}. This effect is greater for larger values of R_{mf}/R_w because the contrast between R_{xo} and R_t is greater. Conversely, when invasion is very shallow, the measurements of so-called R_{xo} microresistivity logs may be affected by the R_t zone.

It may also become very difficult, or impossible, to make accurate corrections for invasion by filtrates of different characteristics. If a mud change is anticipated, the resistivity logs should be run before the change.

Assuming a sharp transition between the R_{xo} and R_t zone, the interpretation problem involves three unknown parameters: R_{xo}, d_i, and R_t. To solve it three different measurements may be required. These preferably include one whose response is affected mostly by R_t, another affected mostly by R_{xo}, and a third affected mostly by variations in d_i.

Determination of R_{xo}

R_{xo} can be determined from the microlaterolog or MicroSFL logs and can sometimes be derived from the microlog or the Proximity log. These pad devices for R_{xo} determination are sensitive to mudcake effects and borehole rugosity, but are usually insensitive to bed-thickness effects.

In the absence of a microresistivity measurement, a value of R_{xo} may be estimated from the porosity using a formula such as

$$R_{xo} = \frac{0.62\ R_{mf}}{\phi^{2.15}(1 - S_{or})^2}, \qquad \text{(Eq. 7-9)}$$

using ϕ from a porosity log and an estimated value of S_{or} (residual oil saturation). In water-bearing formations, this estimate may be good since S_{or} can be fairly safely assumed to be zero. In hydrocarbon-bearing formations, any uncertainty in S_{or} will, of course, be reflected in the R_{xo} estimation from Eq. 7-9.

Resistivity Invasion Corrections

Three resistivity curves of differing depths of investigation can be used to define R_{xo}, R_t, and d_i. These charts have the

appearance of a tornado and are sometimes referred to as "tornado" charts. There are many of these charts, constructed for various combinations of resistivity devices. Some are entered with R_{xo} plus two deeper resistivity log readings; others are entered with three resistivity log values. All provide the information to correct the deep resistivity reading for the effects of invasion, to define the diameter of the invasion, d_i, and to define the R_{xo}/R_t ratio. Those entered with three resistivity measurements also correct the shallow resistivity reading for any deficiencies in invasion and thereby provide an R_{xo} value.

Unless otherwise stated, all invasion correction charts are for thick beds and 8-in. boreholes; readings should be corrected as necessary for bed thickness and hole size. The charts were constructed assuming a step contact between the R_{xo} and R_t zones (no annulus, no transition zone). In most situations this assumption is adequate. In all charts for the induction log, skin-effect corrections have been incorporated.

Charts Rint-3 and -4 make use of R_{xo}, the deep induction (ID or 6FF40), and the LL8 (Chart Rint-3) or SFL (Chart Rint-5) measurements. If the point lies in the plateau region of the curves, it is apparent that invasion is so shallow that $R_{xo}/R_{ID} \cong R_{xo}/R_t$, and $R_{ID} \cong R_t$. These charts take into account the variation in pseudogeometrical factors with R_{xo}/R_t.

Chart Rint-10 makes use of R_{xo}, the deep induction (ID or 6FF40), and the medium induction measurements for the case of $R_{xo} > R_t$.

Charts Rint-9a and -9b are similar charts for the dual laterolog tools, type DLT-B and types DLT-D/E, respectively. They use R_{xo}, LLD, and LLS measurements. Although the correction is moderate at very shallow invasion, the LLD always requires some invasion correction to obtain R_t.

Charts Rint-2a, -2b, -2c use ID, IM, and LL8 or SFL data. Two charts for each set of measurements exist. One is for use when $R_{xo}/R_m \cong 100$ and another for when $R_{xo}/R_m \cong 20$.

Similar charts exist for the Phasor induction combination of IDPH, IMPH, and SFL (Charts Rint-11a,-11b). These apply to 20-kHz tool operation and include the case of $R_{xo} > R_t$. Similar charts are available for 10- and 40-kHz operation. Notice that the Phasor induction tool provides much better resolution in deeper invasion (invasion greater than 50 in.) than does the dual induction tool.

Many oil-base muds will invade the formations and influence resistivity readings. Chart Rint-12 uses the Phasor induction measurements to define R_t and d_i in low-resistivity rocks drilled with such mud. It uses the deep and medium Phasor induction signals after boosting (IDPH and IMPH) and before boosting (IID and IIM).

Compensated Dual Resistivity

The Compensated Dual Resistivity (CDR*) tool[33] is an electromagnetic propagation tool for logging-while-drilling. The CDR tool provides two resistivity measurements with several novel features. These features have been verified by theoretical modeling, test tank experiments, and log examples.

The CDR tool is a 2-MHz electromagnetic propagation tool built into a drill collar. The drill collar is fully self-contained and has rugged sensors and electronics. The measurement is borehole compensated, which requires two transmitters and two receivers. The two transmitters alternately broadcast electromagnetic waves, and the phase shifts and attenuations are measured between the two receivers and averaged. The phase shift is transformed into a shallow measurement, R_{ps}, and the attenuation is transformed into a deep measurement, R_{ad}.

The CDR tool has several new, important features:

- R_{ad} and R_{ps} provide two depths of investigation and are used to detect invasion while drilling. In a 1-ohm-m formation, the diameters of investigation (50% response) are 30 in. for R_{ps} and 50 in. for Rad.
- R_{ad} and R_{ps} detect beds as thin as 6 in. R_{ad} and R_{ps} cross over precisely at the horizontal bed boundaries. This feature can be used to measure bed thickness.
- R_{ad} and R_{ps} are insensitive to hole size and mud resistivity in smooth boreholes. Borehole corrections are very small even for contrasts of 100:1 between formation and mud resistivities (Charts Rcor-11, 12, and 13).

The features of the CDR tool are best demonstrated by field logs. Fig. 7-45 shows the vertical responses for R_{ad} and R_{ps} for a very thin, resistive bed. This well was drilled with an 8.5-in. bit and oil-based mud. Track 1 shows the CDR tool's gamma ray and an EPT attenuation curve and Track 2 shows the measured CDR tool resistivities. The EPT attenuation and the crossovers of R_{ad} and R_{ps} predict a bed thickness of 2 ft.

There are minimal borehole effects in fresh muds, even in large holes. A good example comes from a well drilled in Texas (Fig. 7-46), where the CDR tool logged the same formations with different size holes. The well was drilled with an 8.5-in. bit, reamed once to 17.5 in., and reamed a second time to 26 in. The CDR tool logged the well at 8.5 in. while drilling, and logged the 17.5-in. and 26-in. holes on wiper trips. A Phasor Induction SFL tool logged the 8.5-in. hole. The wireline SP and CDR tool gamma ray are shown in Track 1 (8.5-in. hole). The Phasor induction resistivities are shown in Track 2 and the CDR tool resistivities are shown in Track 3 for the 8.5-in. hole. The CDR tool resistivities for the 17.5-in. hole and for the 26-in.hole are shown in Tracks 4 and 5.

The CDR tool resistivities and the wireline resistivities are in good agreement. Even in the 26-in. hole, R_{ad} reads

the true resistivity because its diameter of investigation is significantly larger than 26 in. However, R_{ps} is more sensitive to the borehole and the vertical sensitivity is reduced because of the large hole size.

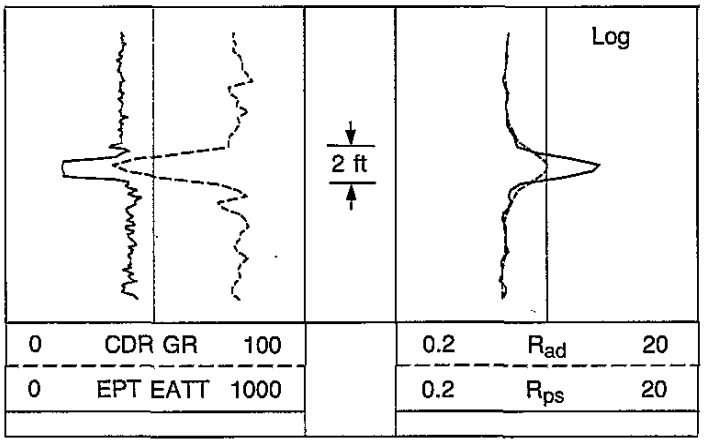

Fig. 7-45—Comparison of CDR tool and the wireline EPT tool response for a thin bed.

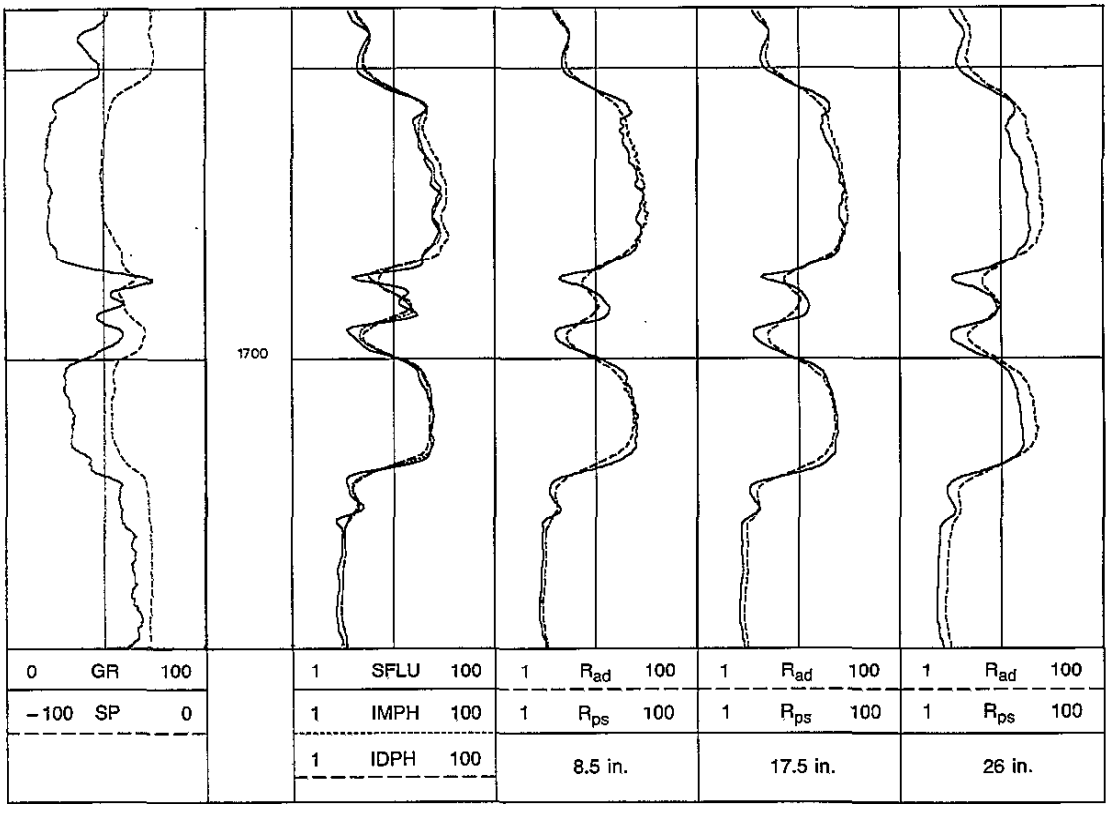

Fig. 7-46—Comparison of CDR tool and Phasor Induction SFL tool of a surface interval showing the effects of borehole size.

Fig. 7-47 shows a case of resistive invasion ($R_{mf} > R_w$) from a well drilled in southern Louisiana. A wireline SP is in Track 1, Phasor Induction tool resistivities are in Track 2, and R_{ad} and R_{ps} are in Track 3. The log shows a series of invaded saltwater sands. Since the mud filtrate is more resistive than the formation water, the IMPH resistivity is higher than the deeper IDPH resistivity. The CDR tool's resistivities reveal a similar profile while drilling. Through most of the upper sand, R_{ps} reads much higher than IDPH, and close to the SFLU. However, the deeper R_{ad} reads close to the IDPH resistivity in these invaded sands. The CDR tool logged these formations 5 to 20 minutes after they were penetrated, while the wireline logs were run about three days later.

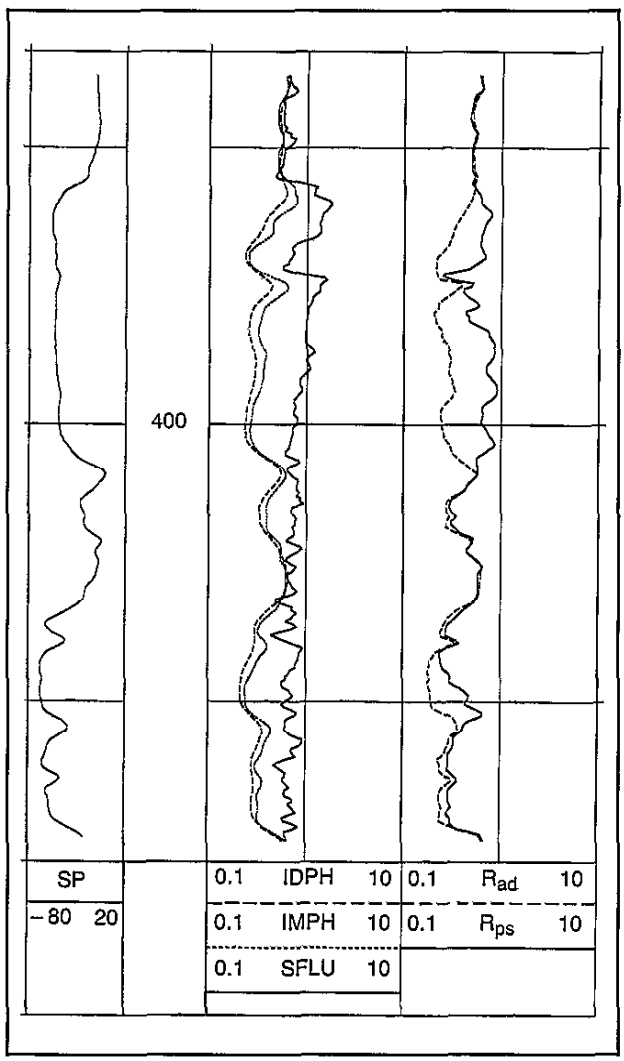

Fig. 7-47—CDR tool and Phasor Induction comparison illustrates invasion.

REFERENCES

1. Schlumberger, C., Schlumberger, M., and Leonardon, E.G.: "Some Observations Concerning Electrical Measurements in Anisotropic Media and Their Interpretation," *Trans.*, AIME (1934) **110**.
2. Schlumberger, C., Schlumberger, M., and Leonardon, E.G.: "Electrical Coring; A Method of Determining Bottom-Hole Data by Electrical Measurements," *Trans.*, AIME (1934) **110**.
3. Schlumberger, C., Schlumberger, M., and Leonardon, E.G.: "A New Contribution to Subsurface Studies by Means of Electrical Measurements in Drill Holes," *Trans.*, AIME (1934) **110**.
4. Lynch, E.J.: *Formation Evaluation*, Harper's Geoscience Series, Harper & Row (1962).
5. Martin, M. and Kunz, K.S.: "Why Those Low Lateral Readings?," *Oil and Gas J.* (Feb. 10, 1958).
6. Doll, H.G.: "The Laterolog," *J. Pet. Tech.* (Nov. 1951).
7. Suau, J., Grimaldi, P., Poupon, A., and Souhaite, P.: "The Dual Laterolog-R_{xo} Tool," paper SPE 4018 presented at the 1972 SPE Annual Meeting.
8. Doll, H.G.: "Introduction to Induction Logging," *J. Pet. Tech.* (June 1949).
9. Dumanoir, J.L., Tixier, M.P., and Martin, M.: "Interpretation of the Induction-Electrical Log in Fresh Mud," *J. Pet. Tech.* (July 1957).
10. Moran, J.H. and Kunz, K.S.: "Basic Theory of Induction Logging," *Geophys.* (Dec. 1962).
11. Tixier, M.P., Alger, R.P., Biggs, W.P., and Carpenter, B.N.: "Combined Logs Pinpoint Reservoir Resistivity," *Pet. Eng.* (Feb.-March 1965).
12. Barber, T.D.: "Introduction of the Digital Dual Induction Tool," paper SPE 12049 presented at the 1983 SPE Annual Technical Conference and Exhibition.
13. Doll, H.G.: "The Microlog," *Trans.*, AIME (1950) **189**.
14. Doll, H.G.: "Filtrate Invasion in Highly Permeable Sands," *Pet. Eng.* (Jan. 1955).
15. Doll, H.G.: "The Microlaterolog," *J. Pet. Tech.* (Jan. 1953).
16. Doll, H.G. and Martin, M.: "Suggestions for Better Electric Log Combinations and Improved Interpretations," *Geophys.* (Aug. 1960).
17. Boyeldieu, C., Coblentz, A., Pelissier-Combescure, J.: "Formation Evaluation in Oil Base Muds," *Trans.*, 1984 SPWLA Annual Logging Symposium.
18. Blakeman, E.R.: "A Method of Analyzing Electrical Logs Recorded on Logarithmic Scale," *J. Pet. Tech.* (Aug. 1952).
19. Barber, T.D.: "Real-Time Environmental Corrections for the DIT-E Digital Dual Induction Tool," *Trans.*, 1985 SPWLA Annual Logging Symposium.
20. Anderson, B.: "The Analysis of Some Unsolved Induction Interpretation Problems Using Computer Modeling," *Trans.*, 1986 SPWLA Annual Logging Symposium.
21. Barber, T.D.: "Invasion Profiling with the Phasor Induction Tool," *Trans.*, 1986 SPWLA Annual Logging Symposium.
22. Frank, Rollyn: *Prospecting With Old E-Logs*, Schlumberger Educational Services, Houston (1986).
23. *Log Interpretation Charts*, Schlumberger Educational Services, Houston (1989).

24. Barber, T. D.: "Phasor Processing of Induction Logs Including Shoulder and Skin Effect Correction," U.S. Patent No. 4,513,376 (1984).
25. Kienitz, C., Flaum, C., Olesen, J-R., and Barber, T.: "Accurate Logging in Large Boreholes," Trans., 1986 SPWLA Annual Logging Symposium.
26. Schaefer, R. T., Barber, T. D., and Dutcher, C. H.: "Phasor Processing of Induction Logs Including Shoulder and Skin Effect Correction," U. S. Patent 4,471,436 (1984).
27. Anderson, B., Safinya, K. A., and Habashy, T.: "Effects of Dipping Beds on the Response of Induction Tools," paper SPE 15488 presented at the 61st Annual SPWLA Technical Conference, October, 1986.
28. Anderson, B., and Barber, T.: "Strange Induction Logs—A Catalog of Environmental Effects," The Log Analyst, XXIX, No. 4, 229-243.
29. Anderson, B., and Barber, T.: "Using Computer Modeling to Provide Missing Information for Interpreting Resistivity Logs," 28th Annual SPWLA Logging Symposium, Texas, June, 1988.
30. Singer, J., and Barber, T.: "The Effect of Transition Zones on the Response of Induction Logs," 28th Annual SPWLA Logging Symposium, June, 1988.
31. Barber, T.: "Induction Log Vertical Resolution Enhancement Physics and Limitations," 28th Annual SPWLA Logging Symposium, June, 1988.
32. *Phasor* Induction Tool*, Schlumberger Educational Services, Houston (1989).
33. Clark, B. *et al.*: "A Dual Depth Resistivity Measurement for FEWD," paper A, 29th Annual SPWLA Logging Symposium, 1988.
34. Anderson, B. and Chew, W.C.: "A New High Speed Technique for Calculating Synthetic Induction and DPT* Logs," paper HH, 25th Annual SPWLA Logging Symposium, 1984.